

Lawrence Berkeley National Laboratory

LBL Publications

Title

Real time side-by-side experimental validation of energy and comfort performance of a zero net energy retrofit package for small commercial buildings

Permalink

<https://escholarship.org/uc/item/6rq3t167>

Authors

Fernandes, Luís L

Regnier, Cynthia M

Publication Date

2022-08-01

DOI

10.1016/j.enbuild.2022.112183

Copyright Information

This work is made available under the terms of a Creative Commons Attribution-NonCommercial License, available at <https://creativecommons.org/licenses/by-nc/4.0/>

Peer reviewed

Real time side-by-side experimental validation of energy and comfort performance of a zero net energy retrofit package for small commercial buildings

Luís L Fernandes, Cynthia M Regnier
Lawrence Berkeley National Laboratory

Abstract

Making buildings zero-net energy (ZNE) is one of the major strategies for achieving carbon emission reduction goals. For this strategy to be successful, it entails a very significant reduction in energy use – 50% or more. In small commercial buildings, however, owners and building management teams usually have limited resources for identifying, analyzing, and procuring appropriate retrofit measures for reducing such use. An approach to overcome this limitation is the development of bundles of energy efficiency measures that can be presented to building owners/operators as a comprehensive package. The research presented in this paper focuses on an experimental evaluation of the impacts of a retrofit package developed for small office buildings in California. Performing this evaluation in a full-scale whole-building integrated systems test facility allowed a side-by-side evaluation in real time, against a reference case, of the impact of the retrofit package not only on energy use but also on visual and thermal comfort. The retrofit package evaluated is comprised of a combination of HVAC, lighting (including daylighting), and plug load measures. The evaluation occurred at different times of the year in order to account for seasonal variations in environmental conditions, including solar angles and weather. The experimental facility allowed testing for two different façade orientations: south and west. Results show that the proposed ZNE retrofit package can save significant amounts of energy for small commercial buildings. During cooling-prevalent periods, total energy savings were 65% for south orientation and 68% for west orientation; during heating-prevalent periods total energy savings were 22% for south orientation and 25% for west orientation. Measurements indicate that the ZNE retrofit package resulted in small but not very significant changes in comfort levels for building occupants.

Keywords

Zero net energy; retrofit; energy conservation measures; energy efficiency; small commercial; office; experimental study

1 Introduction

1.1 Background

Reducing energy use in buildings is key to addressing the ongoing climate crisis through reducing greenhouse gas emissions. In 2020, energy delivered to commercial buildings in the United States amounted to 9.1 EJ, and is projected to grow to 10.9 EJ by 2050 (U.S. Energy Information Administration, 2021). In areas where building replacement rates are low,

retrofitting existing buildings represents a significant opportunity for reducing greenhouse gas emissions from buildings (Zhai et al., 2011). Making buildings zero-net energy (ZNE), i.e., reducing their energy use so that they can be powered by locally-generated renewable energy over a certain period of time (usually annually), is one of the major strategies for achieving carbon emission reduction goals. However, for this strategy to be successful, it entails a very significant reduction in energy use. A Canada Mortgage and Housing Corporation research report mentions that these reductions need to be on the order of 70% to 90% for residential buildings in Canada (Henderson and Mattock, 2007). A ZNE retrofit was expected to achieve a 76% energy use reduction in energy use in a University of Hawai'i building containing classrooms and offices (Regnier et al., 2015). Such a deep reduction in building energy use requires an intervention in the whole building as opposed to individual, incremental equipment upgrades (Regnier et al., 2018).

A wide array of measures and technologies for reducing energy use in large commercial buildings are available. Many of these are also applicable in smaller buildings (less than 4600 m² of floor area), which comprise 50% of commercial building floor space in the United States (U.S. Energy Information Administration, 2020). However, the ownership structure for these smaller buildings often makes it more challenging to achieve large reductions in energy use. In smaller buildings, owners and building management teams usually have less resources for managing building energy use and for identifying, analyzing, and procuring appropriate measures for reducing such use. In small commercial buildings it is therefore fundamental, that the best possible use is made of any opportunities for an energy efficiency retrofit (Sherman et al., 2021). One approach that has emerged to ensure this is the development of bundles of energy efficiency measures that can be presented to building owners/operators as a comprehensive package that can be installed in a single event, thus minimizing costs and disruption to building operations.

Prior to the experiment presented here, a ZNE retrofit package was developed for small commercial buildings in California (Regnier et al., 2020). The process for developing the retrofit package involved a preliminary evaluation, using computer simulation, of different combinations of energy efficiency measures targeted at achieving 5% internal rate of return (IRR) over 10 years and 30% energy savings over “business as usual” (BAU) retrofits that met the 2016 version of the California building energy code (California Energy Commission, 2015). The final package contained a combination of HVAC, lighting (including daylighting), and plug load measures. Measures aimed at the building envelope were also considered but did not meet the cost-effectiveness targets. Table 1 shows a comparison of retrofit costs between ZNE and two BAU retrofit packages as implemented in a two-story, 4647 m² building in a northern California location, using local labor rates. The lower cost of the ZNE package can be attributed to lower HVAC system costs; these are due to building improvements that lowered the heating and cooling peak demands such that smaller equipment (and ducting) could be utilized. It should be noted that the ZNE package cost does not include the cost of a photovoltaic system, which would be needed to complement the package. The main focus of the analysis was to assess the cost aspects of the retrofit component only. Table 2 describes the assessed energy performance and costs of the three cases for the 4647 m² building example. Overall, the ZNE

package, which also happened to be carbon neutral, had a lower annual energy cost than BAU2, but a higher energy cost than BAU1. Some of these cost differences could be attributed to the relative low cost of natural gas in this region, as compared to electricity. The IRR for each package is presented in Table 3, assuming a 30-year life cycle, a 10% interest rate, and an energy cost escalation rate of 3% per year. Given that the ZNE package had a lower installation cost than BAU1 and BAU2, the payback is immediate, requiring no cost recovery period. This initial capital cost savings will offset any increase in utility costs (as compared with BAU1), but only further improves the overall financial position over BAU2.

Table 1. Total retrofit costs for business as usual (BAU) and ZNE packages.

Package	Configuration	Total retrofit cost (million US dollars)
BAU1	Packaged single zone rooftop air conditioner units, with gas heat, lighting upgrades (fixtures and controls), domestic hot water heater replacement, roof replacement (considering end of life of roof materials), and incidental related costs such as ducting, testing and balancing costs	1.728
BAU2	Variable air volume rooftop unit, with hydronic boiler, serving VAV reheat boxes in each zone, lighting upgrades (fixtures and controls), domestic hot water heater replacement, roof replacement (considering end of life of roof materials), and incidental related costs such as ducting, testing and balancing costs	1.828
ZNE	Heat pump with variable refrigerant flow, dedicated outdoor air system, plug load reduction, lighting upgrades (more efficient than BAU), domestic hot water heater replacement, roof replacement (considering end of life of roof materials), and incidental related costs such as ducting, testing and balancing costs	1.277

Table 2. Annual energy consumption and energy costs for business as usual (BAU) and ZNE packages.

Package	Annual electricity consumption (kWh)	Annual gas consumption (kWh)	Annual energy cost (US dollars)
BAU1	303314	280841	70222
BAU2	337739	404750	81766
ZNE	389598	Not applicable	79994

Table 3. Cost-effectiveness indicators for the ZNE package using incremental retrofit costs.

Package	Internal rate of return (IRR)	Net present value (NPV) (thousand US dollars)	Simple payback (years)
ZNE	Capital positive	780	-9

The ZNE retrofit package is applicable to buildings that are divided into small spaces or have small windows, thus requiring skylights as a solution for illuminating interior spaces. The interior of small commercial buildings is often organized into smaller spaces, with limited daylight availability beyond the spaces that happen to be illuminated by windows, which may or may not be of substantial size, especially in older buildings. Skylights are a tried and tested way of bringing daylight to interior spaces; in recent decades, tubular daylight devices (TDDs) have emerged as a viable option to achieve substantial levels of daylight illumination while minimizing the negative thermal impacts of an envelope opening on the roof (Malet-Damour, 2019). Another advantage of the minimal roof area TDDs require when compared with

conventional skylights is the fact that they leave a higher proportion of roof area available for solar collection by photovoltaic panels; this is particularly important when attempting to reach zero net energy building operation.

1.2 Evaluating the performance of retrofit packages

The performance of packages of energy efficiency measures does not necessarily amount to adding up the impact of each individual measure, as there are interactive effects between measures to take into account (Chidiac et al., 2011). When developing such packages, it is then crucial to carefully evaluate their performance as a whole. The abundant literature on experimental evaluations of individual energy efficiency measures for commercial buildings is therefore of limited usefulness here due to these interactive effects.

Experimental evaluations of retrofit packages in commercial buildings are usually structured as a case study in an existing building, in which energy and occupant-related variables are assessed before and after the retrofit, often using different methods. The small office retrofit presented by Dean and Turnbull is a typical example of the latter approach, where the original energy use was estimated using a generic building simulation model whereas the post-retrofit energy use was measured (Dean and Turnbull, 2014). The New Buildings Institute, in its Getting to Zero Buildings Database, presents several retrofit case studies where the pre-retrofit energy use is estimated using a combination of measurements and simulation (New Buildings Institute, 2021). One challenge with such evaluations is that, even if they rely on measurements for both pre- and post-retrofit situations, several factors that influence energy use can change simultaneously with the retrofit measures. The weather, the level of occupancy in the space, and the way the space is utilized are not guaranteed to stay the same during the pre- and post-retrofit evaluation periods. Furthermore, the fact that these are buildings in regular operation also limits the type and duration of measurements that can be performed, due to the need to not interfere with such operation or disturb occupants.

It is widely accepted that software tools that include building simulation provide a computational route to avoid these issues. Software tools specifically devoted to retrofits in commercial buildings can simplify the process of developing suitable retrofit packages, as was done prior to the experiment presented in this paper (Lee et al., 2015). The ability to obtain indicative results at low cost and with minimal risk is especially valuable in the design and planning stages of new buildings or retrofits in existing buildings. However, due to the idiosyncrasies of building construction and operation it can be challenging to guarantee that actual energy savings will match simulation results for a particular building and climate (Hu and Milner, 2021).

The limitations of pre-/post-installation comparisons and building simulation can be overcome when performing measurements in a full-scale laboratory setting that allows for real-time, side-by-side comparison between pre- and post-retrofit conditions. This type of facility exists in only a relatively small number of research institutions. Possibly as a result of this, the literature on laboratory experiments explicitly aimed at evaluating comprehensive retrofit packages (i.e., including such diverse building systems as HVAC, lighting, and plug loads) is scarce. However, a

few recent experiments have begun to address this research gap. Mathew et al. evaluate a retrofit package aimed at specific points in the real estate life cycle that centered around lighting and HVAC, with the optional addition of ceiling fans, automated shading and some plug load controls, achieving a combined savings of 33-40% (Mathew et al., 2020). Shackelford et al. studied integrated lighting and shading system retrofits, achieving up to 70% energy savings (Shackelford et al., 2020). So far, the physical layout of these experiments mimicked a typical open-plan office configuration, with a focus towards medium and large office buildings.

Comparable experimental data for small commercial buildings, with their idiosyncratic ownership structure and which are often densely partitioned and therefore where the daylight from windows doesn't reach beyond one relatively small room, is not available in the literature. While some of the available research data may be applicable, the retrofit packages evaluated in the existing literature were not developed specifically for small commercial buildings, with some features that might not be within the economic reach of a small building owner/operator. Equivalent experimental data is needed in order to more accurately quantify the benefits of retrofit packages specifically aimed at small commercial buildings.

1.3 Study objectives

The research presented in this paper is a careful real-time, side-by-side experimental evaluation of the impacts of a retrofit package specifically developed for helping achieve ZNE small office buildings in California (Regnier et al., 2020). Real time measurements include not only impacts on energy use but, importantly for occupant acceptability, also impacts on visual and thermal comfort. This study addresses the lack of experimental data on the side-by-side energy and comfort performance of retrofit packages that are cost-effective specifically for small commercial buildings, with a high level of space partitioning and hence limited availability of daylight from windows across the floorplan.

The following section of this paper details the evaluation methodology, followed by a section containing the main results. The two final sections contain a discussion of some aspects of the results, addressing their applicability beyond the specific location where the experiment was conducted, and more general conclusions to be drawn from the study. A fuller set of results is in the supplementary material included with this paper.

2 Method

The performance of the zero net retrofit package was evaluated experimentally at full scale in a whole-building integrated systems test facility (FLEXLAB, Lawrence Berkeley National Laboratory, 2020) in Berkeley, California, United States. This facility has several testbeds each consisting of two identical, calibrated test cells that enable detailed comparative evaluations under controlled conditions. The study presented here was performed in a testbed that is able to rotate, allowing tests for more than one façade orientation.

Quantities measured in the experiment included several aspects of energy use and occupant comfort (Table 4); some quantities, such as lighting energy use, were directly measured,

whereas others required calculation based on directly measured quantities and additional data. More detail is presented in the rest of this section.

Table 4. Overview of measurements performed and quantities indirectly derived from measurements

		Direct measurements	Calculated quantities	Notes
Energy	HVAC	Space cooling and heating loads	Cooling and heating energy use	Energy used derived from loads by using EnergyPlus modeling input data and equations
		Fan energy use	-	
	Lighting	Electrical load	-	
	Plug loads	Electrical load	-	
Comfort	Thermal	Air temperature Mean radiant temperature	Predicted Mean Value (PMV) Predicted Percentage Dissatisfied (PPD)	For the PMV/PPD calculation, relative humidity and air velocity were derived from subsequent measurements in the same facility and manufacturer data, respectively
	Visual	Luminance mapping	Daylight Glare Probability (DGP)	

2.1 Test configurations

Both test cells were configured to emulate office environments. One cell (*ZNE cell*) was set up to mimic an office space retrofit with an array of ZNE energy efficiency measures; the other cell (*reference cell*) was set up to represent a common existing small office building (Table 5, Figure 1 to Figure 4). Each cell was divided into three spaces, using foam partitions that restricted air movement and light transmission, in order to represent typical dimensions for office spaces in small commercial buildings. The partitions were finished with the same paint used for the test cell walls. Throughout the paper, the space by the window will be referred to as the *window space*, the enclosed space in the middle as the *middle space*, and the space at the back of the cell (if one thinks of the window as the front) as the *back space*.

Table 5. Test configurations.

Orientation	ZNE cell	Reference cell
South	<ul style="list-style-type: none"> • HVAC: variable refrigerant flow, dedicated outdoor air system, wide deadband, setbacks/shutoff when space unoccupied, modulating supply diffusers • Façade: <ul style="list-style-type: none"> ○ WWR 0.25 	<ul style="list-style-type: none"> • HVAC: packaged variable air volume with hydronic coils, gas furnace, static supply diffusers • Façade: <ul style="list-style-type: none"> ○ WWR 0.25 ○ Clear, single-pane window w/ thermally broken (single break) aluminum frame

Orientation	ZNE cell	Reference cell
	<ul style="list-style-type: none"> ○ Clear, single-pane window w/ thermally broken (single break) aluminum frame ○ metal stud wall w/ 3.35 K m²/W batt cavity insulation • Roof: 3.52 K m²/W continuous insulation • Other walls: <ul style="list-style-type: none"> ○ Back wall: 5.14 K m²/W continuous insulation ○ Side walls: > 8.4 K m²/W (exterior wall), > 12 K m²/W (wall between cells) • Lighting: 4.3 W/m², LED, occupancy sensing, daylight harvesting • Plug loads: 5.8 W/m² connected load 	<ul style="list-style-type: none"> ○ metal stud wall w/ 3.35 K m²/W batt cavity insulation • Roof: 3.52 K m²/W continuous insulation • Other walls: <ul style="list-style-type: none"> ○ Back wall: 5.14 K m²/W continuous insulation ○ Side walls: > 8.4 K m²/W (exterior wall), > 12 K m²/W (wall between cells) • Lighting: 12.8 W/m², 3-lamp T8 fluorescent recessed luminaires • Plug loads: 8.3 W/m² connected load
West	West orientation; all else same as above	West orientation; all else same as above

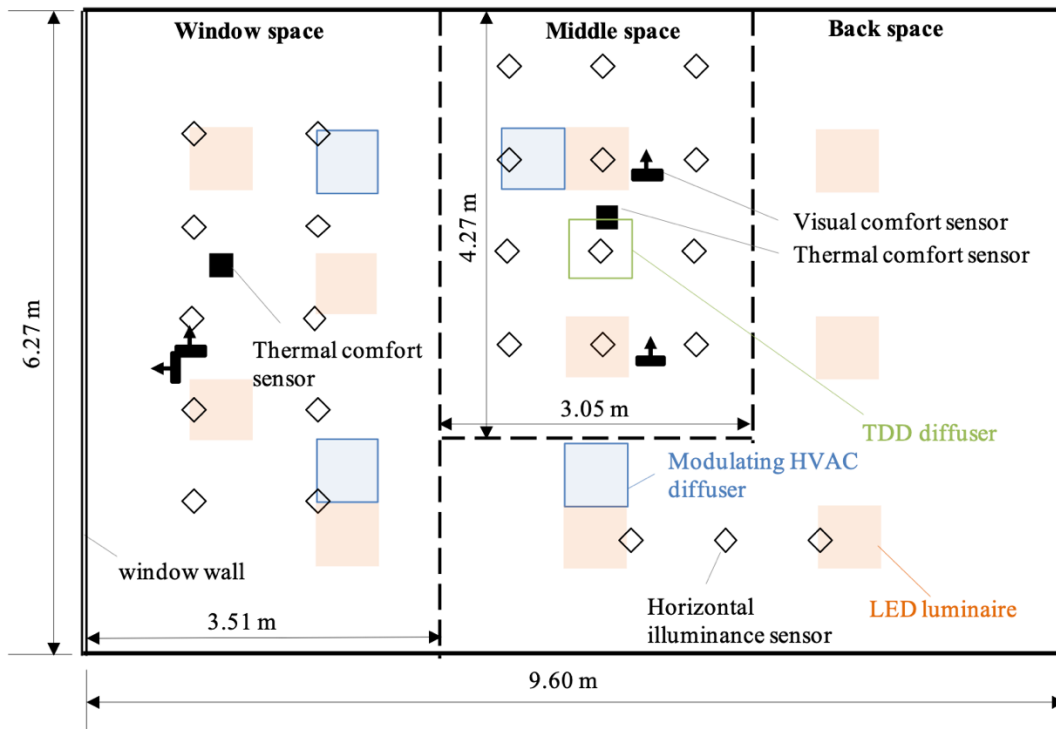


Figure 1. Experimental configuration in ZNE cell.

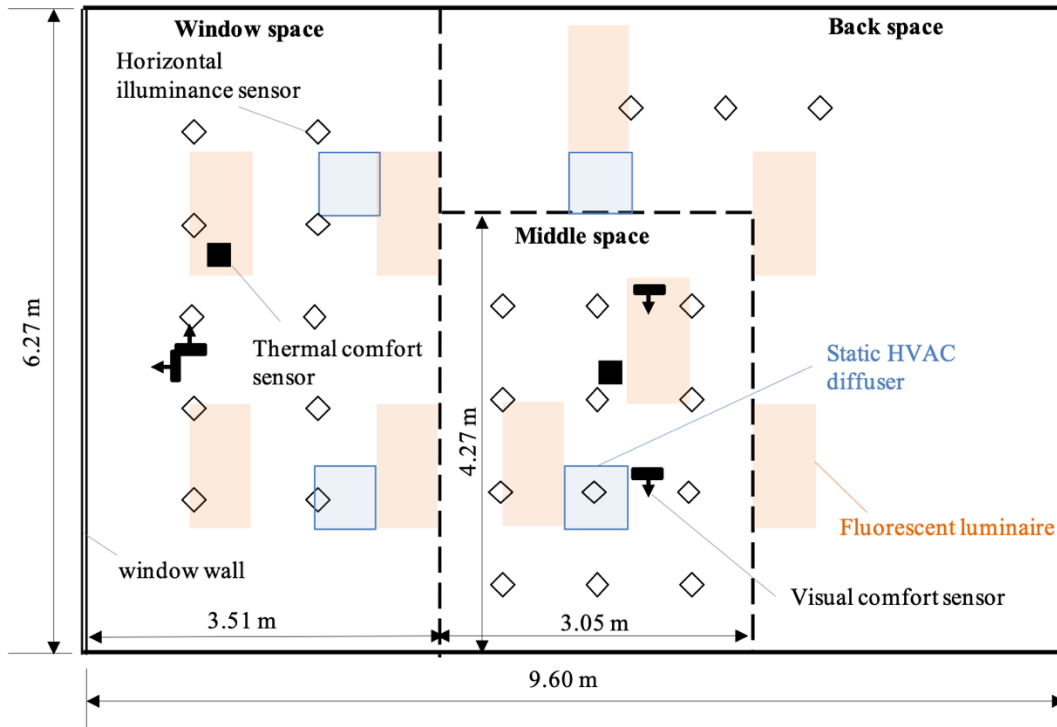


Figure 2. Experimental configuration in reference cell.



Figure 3. Aspect of window (image on the left) and middle (image on the right) spaces of ZNE cell.



Figure 4. Aspect of window (image on the left) and middle (image on the right) spaces of reference cell.

2.1.1 Building systems

2.1.1.1 HVAC

The testing facility's HVAC system was configured to best approximate the performance of the ZNE and reference HVAC systems. In both systems, the air handling unit (AHU) was programmed for an occupied schedule of 7 AM to midnight on weekdays (Monday to Friday), 7 AM to 7 PM on Saturdays, and 7 AM to 6 PM on Sunday. In both AHUs the following variables were monitored: supply air flow, supply and return air temperatures.

2.1.1.1.1 ZNE cell

The HVAC system considered for the ZNE configuration consisted of a rooftop, 100% outside air high efficiency heat pump (COP of 3.3), with energy recovery on the relief air. The controls strategy allowed for space conditioning through the use of the outside air only unit, while allowing for a larger deadband for heating and cooling setpoints.

The air handling unit (AHU) had a variable frequency drive fan, and supplied air to modulating supply diffusers (MSD), (Thermafuser model TF-HC, (Acutherm, 2020)). The ZNE cell AHU was configured for 100% outside air operation only, with no recirculation. Supply fan speed was controlled to maintain duct static pressure at setpoint when the fan was proven on. AHU supply air temperature control loops were enabled when the supply fan was proven on, and disabled with output set to zero (no heating, no cooling, no heat recovery) otherwise. The AHU was scheduled for a 25.6°C cooling setpoint, and a 21.1°C heating setpoint. The supply air temperature setpoints were as follows: the minimum and maximum for cooling were 12.8°C and 20.0°C, respectively; the minimum and maximum for heating were 24.4°C and 35.0°C, respectively. The ductwork was generally sized for a pressure drop of 65.4 mPa/m of straight duct.

The MSDs enabled VAV control at the diffuser. They have an internal damper that is modulated closed or open depending on the mode of operation of the air handling system (heating or cooling), and the thermostatic setpoints provided at the diffuser. The model used in this

experiment had thermally actuated dampers, where a wax product expands or contracts to modulate the damper open or closed depending on the desired setpoints, which can be set manually at the damper. The advantage of these diffusers is that they may provide more granular temperature control in workspaces when compared with single zone control. In addition, by design they require a lower pressure drop duct design, which improves fan energy performance throughout all modes of operation. For this experiment, the wax cylinder thermostats on each MSD were set to setpoints of 20.0°C and 25.6°C for heating and cooling mode respectively.

2.1.1.1.2 Reference cell

The reference cell AHU was configured to emulate a gas packaged direct expansion air handler (cooling COP of 2.7), with no economizer, no demand-based ventilation and no energy recovery on the relief air. Minimum airflow was set to 30% of maximum airflow. The AHU was scheduled for a 23.9°C cooling setpoint, and a 21.1°C heating setpoint. The supply air temperatures were 12.8°C and 35.0°C for cooling and heating, respectively. Supply diffusers were conventional (i.e., non-modulating) ceiling diffusers, with ductwork generally sized for a pressure drop of 81.8 mPa/m of straight ductwork.

2.1.1.2 Lighting

The lighting systems implemented in the testing facility were designed to match the specifications in the test and reference configurations.

2.1.1.2.1 ZNE cell

In the ZNE cell, electric lighting was provided by ten 61 x 61 cm recessed LED luminaires (Philips Spacewise), each rated at 26 W (Figure 5). Each of these luminaires has a passive infrared occupancy sensor and a photosensor, and can autonomously dim or turn off based on available daylight and/or detected occupancy. Luminaires can be grouped so their response to occupancy and/or available daylight is the same within the group. For this experiment, luminaires were set to dim individually according to available daylight, but to respond as a group when occupancy was detected. A device was constructed, using a heat source, a table fan and a timer, that would trigger one of the occupancy sensors in order to approximate the desired occupancy schedule (Table 6, derived from Table G-1 in (ASHRAE, 2008)).



Figure 5. Luminaires used in the tests: LED luminaire used in the ZNE cell (left) and fluorescent troffer used in the reference cell (right).

Table 6. Occupancy schedule.

Hour	Occupancy		
	Weekday	Saturday	Sunday
0	0%	0%	0%
1	0%	0%	0%
2	0%	0%	0%
3	0%	0%	0%
4	0%	0%	0%
5	0%	0%	0%
6	10%	10%	5%
7	20%	10%	5%
8	95%	30%	5%
9	95%	30%	5%
10	95%	30%	5%
11	95%	30%	5%
12	50%	10%	5%
13	95%	10%	5%
14	95%	10%	5%
15	95%	10%	5%
16	95%	10%	5%
17	30%	5%	5%
18	10%	5%	5%
19	10%	0%	0%
20	10%	0%	0%
21	10%	0%	0%
22	5%	0%	0%
23	5%	0%	0%

The middle space of the ZNE cell was also illuminated by a 53.3-cm diameter TDD (Solatube 750 DS-C), with a prismatic exterior dome and a 61 x 61 cm Fresnel-type optical ceiling-mounted diffuser (Figure 6). The length of tube between the dome and the diffuser was 1.65 m.

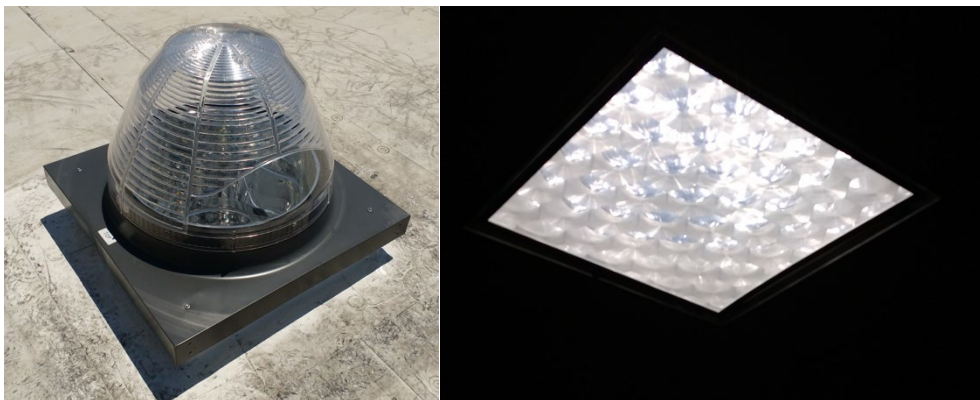


Figure 6. Prismatic dome (left) and Fresnel-type ceiling-mounted diffuser (right). Note that, in order for the optical structure of the diffuser to be visible in the image, the interior ceiling was underexposed and appears black.

2.1.1.2.2 Reference cell

Nine 61 x 122 cm three-lamp fluorescent troffers provided electric lighting to the reference cell. These luminaires were fitted with 32-W fluorescent lamps that had been seasoned for at least 100 hours. In order to better match the desired lighting power density of 12.8 W/m², a non-lighting 70 W load was added to the lighting circuits. Reference cell lights were on from 7 AM to midnight on weekdays and 7 AM to 7 PM on weekends.

2.1.2 Occupant-related loads

2.1.2.1 Occupant generated heat

The spaces were assumed to be occupied according to Table 6. To provide the appropriate amount of occupant generated heat to the space, heat generating devices (the white, vertical cylinders visible in Figure 3 and Figure 4) operated by timers were placed throughout both ZNE and reference cells. An occupant density of 18.6 square meters per occupant was assumed, and an occupant-generated power of 130 watt per occupant, corresponding to moderately active office work (ASHRAE, 2001).

2.1.2.2 Plug loads

Plug loads (e.g., from office equipment) were simulated using desktop personal computers running CPU-intensive tasks on a schedule so that their electricity consumption matched the desired load profile and the power density shown in Table 5.¹ The 30% reduction in power density between the reference and ZNE cells assumed the use of “smart” occupancy-controlled plug strips, laptops instead of desktop computers, replacement of equipment and appliances with high efficiency (e.g., EnergyStar) models, the consolidation of office equipment such as printers and fax machines to a common branch electrical panel with a power off control, and virtualizing or moving computer servers offsite.

2.2 Measurements

2.2.1 HVAC

Each AHU was served by individual hot and chilled water coils in which the flow rate (Siemens Sitrans FM MAG 3100, °C for velocities ≥ 0.09 m/s), supply temperature and return temperature (platinum resistance temperature detector, ±0.031°C) were monitored. These data allowed the calculation of the amount of heat supplied to or removed from each cell. The site energy (electric and/or gas) needed to provide the measured amounts of heating and cooling was then calculated based on the efficiency characteristics of the equipment assumed for each cell’s configuration.

In the reference cell, the efficiency parameters used to convert measured thermal loads into electricity use were derived from an EnergyPlus model of a Daikin DPS006A single-zone, variable air volume (VAV) heat pump with an 0-100% economizer with comparative enthalpy

¹ In some instances, some equipment with low power consumption, such as sensors for monitoring visual comfort, was connected to the same circuits that powered the desktop computers that simulated generic plug loads. Because the way in which this low-power equipment was connected to circuits was not completely consistent between tests, this introduced minor between-test variations in the actual plug loads on the measured electrical circuits. These variations were not expected to have a significant effect on the overall test results.

control. EnergyPlus is generally recognized as one of the standard software packages for whole-building energy simulation. The EnergyPlus parameters were used according to the specifications in the EnergyPlus Engineering Reference manual (EnergyPlus, 2018). In the reference cell, a similar process was performed for the reference, conventional HVAC system; for heating, a constant furnace efficiency of 80% was assumed.

2.2.2 Electrical loads

For each cell, lighting and plug loads were measured by current transducers (Verivolt Envoy-AC, $\pm 0.2\%$) at the electrical panel for each circuit. Lighting loads for the window, middle, and back spaces were connected to a dedicated electrical circuit and therefore monitored separately.

2.2.3 Thermal comfort

Thermal comfort was evaluated using the Predicted Mean Vote/Predicted Percentage of Dissatisfied (PMV/PPD) framework (ASHRAE, 2013). PMV is a value between -3 and 3 and indicates how occupants are likely to perceive the space: values of -3, -2, -1, 0, 1, 2, 3 correspond to perceptions of the space as “cold”, “cool”, “slightly cool”, “neutral”, “slightly warm”, “warm”, and “hot”, respectively. PPD represents the percentage of people who would not be satisfied with the measured thermal environment. In order to achieve comfortable conditions, it is recommended that PPD be maintained under 20% and PMV between -0.5 and 0.5. PMV and PPD are calculated based on environmental variables such as air temperature, mean radiant temperature, air velocity, and relative humidity, as well as assumptions about 1) the occupants’ metabolic rate, determined by the type of physical activity that occupants are assumed to be engaged in, and 2) the insulation provided by the clothing that the occupants are assumed to be wearing.

In this study, the PMV/PPD calculation method prescribed by the ASHRAE standard was followed as much as possible, with a few simplifications and assumptions detailed further down in this section. These were motivated mainly to the fact that the main priority in this experiment was not the measurement of absolute levels of thermal comfort in conformance to the standard, but the determination of whether the expected energy use reductions in the ZNE cell relative to the reference cell would happen at the expense of thermal comfort. Secondly, some assumptions were also dictated by challenges with the availability and reliability of some measuring equipment.

Dry bulb and mean radiant temperature were measured in the window and middle spaces, with sensors placed on the desktops ($\pm 0.1^\circ\text{C}$ accuracy; sensors placed 1.01 m above the floor), using thermal comfort measurement stations like the one shown in Figure 7. These temperature measurements are somewhat simplified relative to what ASHRAE 55 prescribes (e.g., air temperature at desk height versus an average of temperatures at 0.1, 0.6, and 1.1 m above the floor for seated occupants); as mentioned above, they are intended here as a practical simplification, intended for comparing thermal comfort between the two cells.

At the time of this experiment, equipment for measuring relative humidity was not available in the experimental facility. Relative humidity measurements performed at the same time of the year during similar experiments between December 2019 and August 2020 were used to derive

typical relative humidity levels for each test: 42.5%, 42.5%, 47.5%, and 32.5% were used for May, June, August, and December, respectively.

Air velocity was estimated from manufacturer data sheets for both types of diffusers (MSD data was used for the ZNE cell and conventional diffuser data for the reference cell), based on the distance between each thermal comfort station and the nearest diffuser².

An occupant metabolic rate of 1.3 met was assumed; this can be considered an average value for office work (Akimoto et al., 2010). Clothing levels were assumed to be 0.61 clo (trousers, long-sleeved shirt, according to the CBE ASHRAE-55 Thermal Comfort Tool (University of California, Berkeley, 2021)) for cooling-prevalent periods and 1.00 clo (typical winter indoor clothing (University of California, Berkeley, 2021)) for heating-prevalent periods.

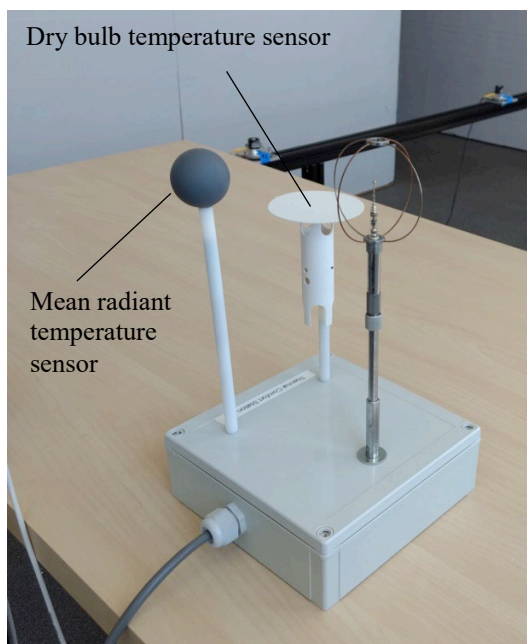


Figure 7. Thermal comfort measuring station.

2.2.4 Visual comfort

Visual comfort was measured using high-dynamic-range (HDR) luminance mapping techniques and the Daylight Glare Probability (DGP) metric (Wienold and Christoffersen, 2006). HDR images were captured using digital single-lens reflex cameras fitted with fisheye lenses, auxiliary sensors and computing equipment (Figure 8). These HDR images were processed in order to calculate a luminance map of the image, i.e., calculate the luminance of each pixel. A false-color luminance map from the experiment is shown in Figure 9.

² The reader may note that the thermal comfort station shown in Figure 7 also displays an air velocity sensor. Some of these sensors malfunctioned during the experiment and therefore their data was excluded from the analysis presented here.



Figure 8. High-dynamic-range luminance mapping apparatus for glare measurements.

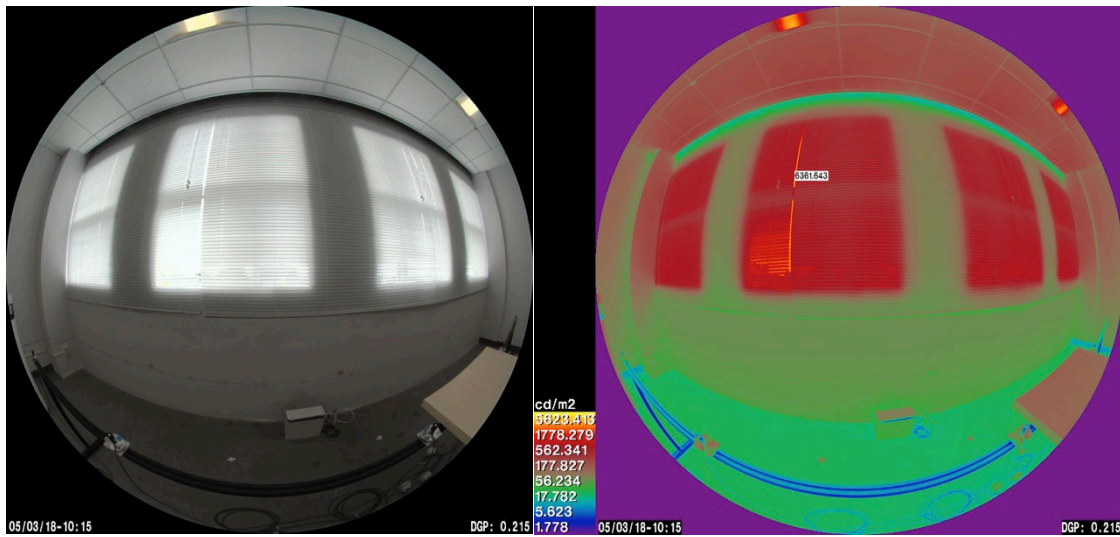


Figure 9. HDR image (left) and corresponding luminance map (right) of scene in FLEXLAB.

The DGP metric represents a probability, between 0 and 1, that occupants of the space will experience glare when their eyes are at the position of the camera lens at the time that the HDR image was captured. Subjective ratings corresponding to DGP values are as follows: 0.30, 0.35, 0.40 and 0.45 are the thresholds for “just imperceptible glare” “just perceptible glare”, “just disturbing glare” and “just intolerable” glare. In general, it is desirable that DGP remains

below 0.35, and that breaches above that level are of short duration and do not exceed 0.40. The accuracy of the DGP measurement is estimated at $\pm 10\%$.

2.2.5 Light levels

Horizontal illuminance was measured using Licor LI-210 photometers ($\pm 5\%$ accuracy), mounted 76 cm above the floor, and leveled. Figure 10 shows one of these photometers mounted on a stand inside one of the test cells. Horizontal illuminance data was used for assessing light levels within the space.

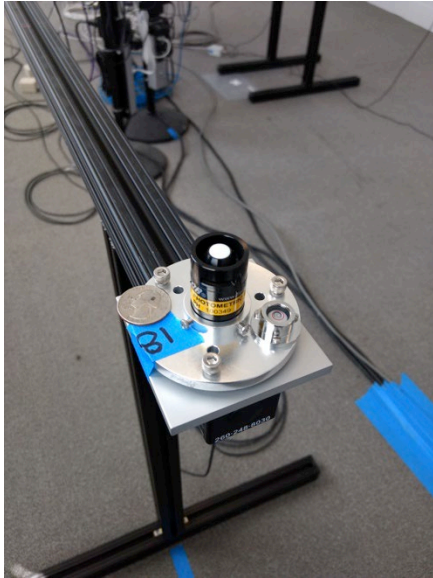


Figure 10. Photometer on stand inside test cell.

2.2.6 Outdoor environmental conditions

The outside air temperature was measured by a weather station (measurement accuracy $\pm 0.1^\circ\text{C}$) located at the facility where the experiment took place. Exterior global and diffuse horizontal irradiance were available from a weather station (Hukseflux SR12, $\pm 3\%$) in a nearby research facility, situated approximately 300 m from the test cells. Data from prior experiments indicated that the difference between these data and data gathered at the test cell location was insignificant.

2.3 Test calendar

Measurements were conducted during four periods spread out throughout the year. This accounted for seasonal variations in environmental conditions, including solar angles and weather. Dates for the four test periods were partly determined by the availability of the shared experimental facility and are shown in Table 7.

Table 7. Dates for conducted tests.

Orientation	Test period 1	Test period 2	Test period 3	Test period 4
South	May 3 - May 10	Jun 13 - Jun 19	Aug 18 - Aug 24	Dec 5 - Dec 11
West	May 11 - May 17	Jun 20 - Jun 26	Aug 25 - Aug 31	Dec 13 - Dec 20

3 Results

This section includes the main results from the experiment presented in this paper. Tables and plots further detailing results from each test period are included in the Appendix.

3.1 Energy use

3.1.1 Plug Loads

Overall, plug load energy use was 31% lower in the ZNE cell than in the reference cell (88 versus 127 kWh). Figure 11 and Figure 12 show plug load electrical energy consumption during a typical weekday and on weekends, respectively. These results are in line with the differences in connected plug load density between the two cells as noted in Table 5: 5.8 W/m² in the ZNE cell versus 8.3 W/m² in the reference cell. Between tests, minimal variation was observed in plug load energy consumption for the same cell. The small variations that did occur were due to inconsistent connection of low power equipment such as cameras for monitoring visual comfort; this effect did not affect the outcome of the experiment because it was much smaller than the between-cell difference in plug load electricity consumption.

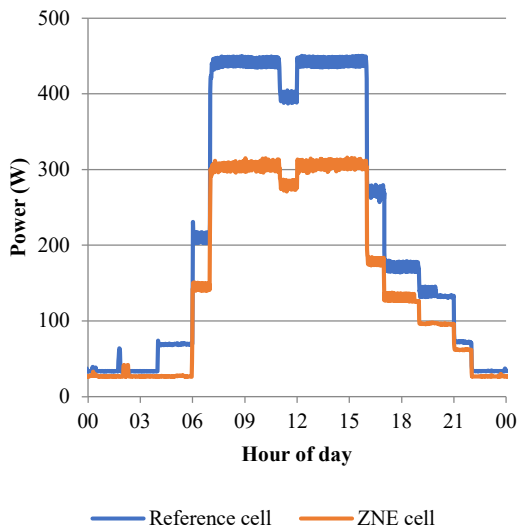


Figure 11. Plug load energy consumption for typical weekday.

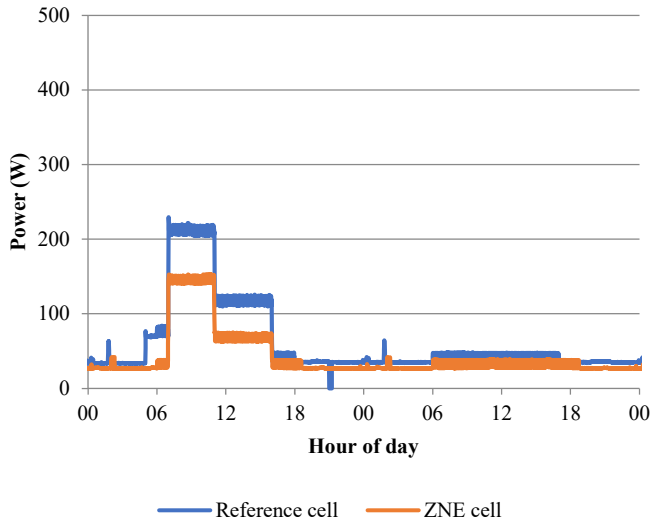


Figure 12. Plug load consumption for typical weekend.

3.1.2 Lighting

Lighting energy consumption throughout the four testing periods was significantly lower in the ZNE cell than in the reference cell (see Figure 13 and Figure 14 for typical weekday energy consumption during the four tests). For south orientation, and when taking the four tests together, total lighting energy use was 85% lower in the ZNE cell when compared to the reference cell. Similarly, for west façade orientation the lighting energy use reduction was also 85%. When analyzing lighting energy use by each of the three spaces into which each cell was divided, lighting energy use reduction was 90%, 89% and 76% for the window, middle and interior spaces, respectively, for south orientation; for west orientation the corresponding values were very similar: 90%, 89%, 77%. These significant reductions in lighting energy use are a cumulative result of lowering the connected lighting power density and introducing daylight harvesting and occupancy controls, in combination with the expansion of the daylit floor area through the addition of TDDs.

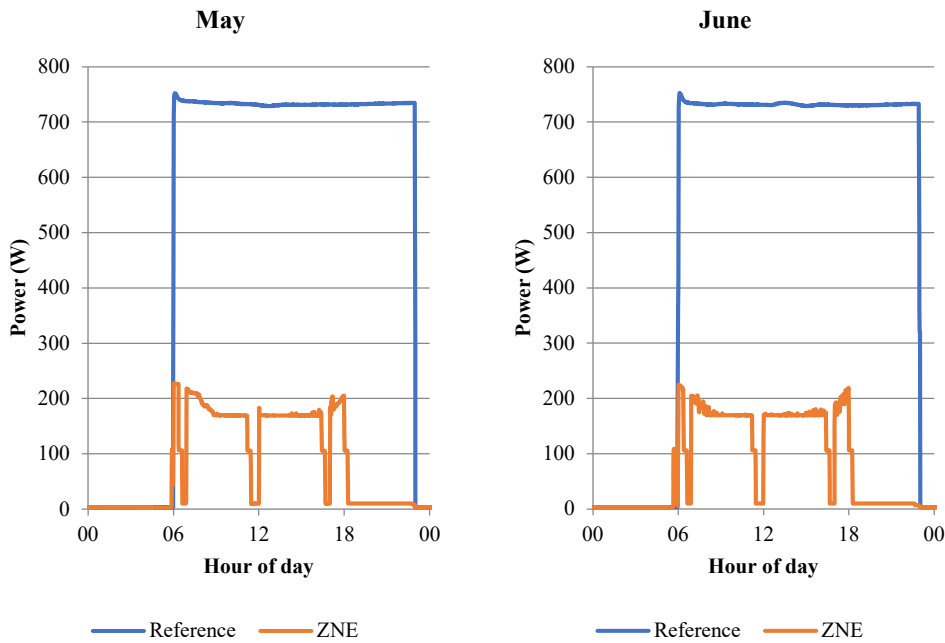


Figure 13. Lighting power consumption on typical weekdays for Test 1 (May) and Test 2 (June).

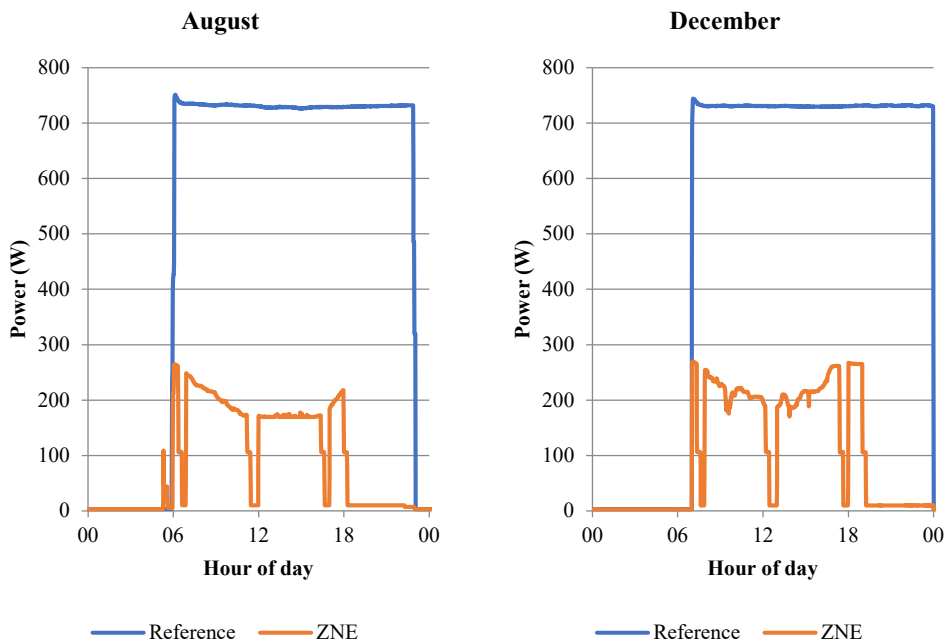


Figure 14. Lighting power consumption on typical weekdays for Test 3 (August) and Test 4 (December).

3.1.3 HVAC

3.1.3.1 Thermal loads

The distributions of the measured outside air temperature and solar radiation are shown in Figure 15, using a kernel-density estimator to derive a probability function from weather data gathered in the vicinity of the test facility. While the relatively mild climate does not have

extreme between-season variations in temperature and solar radiation availability, June (Test 2) and December (Test 4) have respectively the highest and lowest mean outside air temperature and global horizontal irradiance, with the other tests occurring with intermediate environmental conditions between those two.

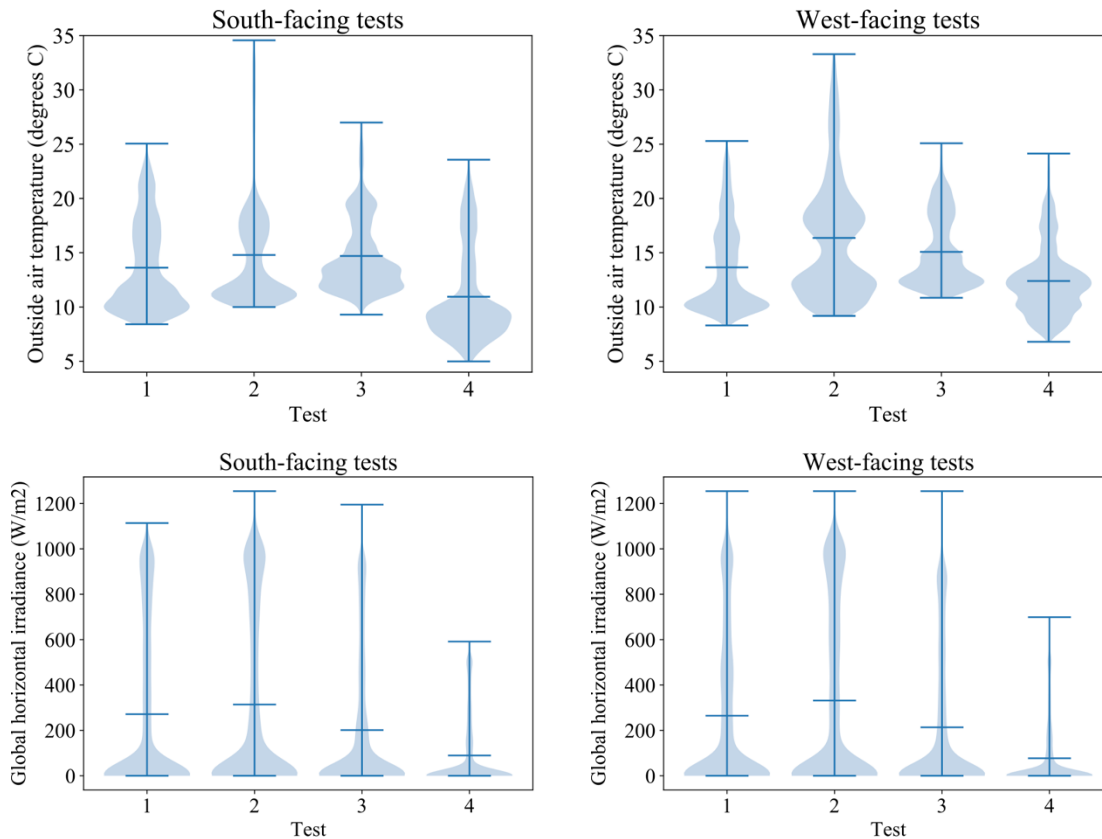


Figure 15. Kernel-density estimator distribution plots of outside air temperature and global horizontal irradiance for the four test periods. In each plot the horizontal blue lines denote the extrema and the mean of the data.

The HVAC system in the reference cell was in cooling mode most of the days during Tests 1-3, whereas the ZNE cell showed moderate levels of both heating and cooling (Figure 16 to Figure 19). For these periods, overall HVAC thermal energy use³ was significantly lower in the ZNE cell than in the reference cell. For south orientation, the total HVAC thermal energy use was 290 and 62 kWh for reference and ZNE cells, respectively, representing a savings of 79%. For west orientation, the corresponding values were 353 and 66 kWh, representing 81% savings.

Test 4 (December) showed significantly different energy use patterns, with the reference cell in both heating and cooling mode and the ZNE cell only heating (Figure 19). During this period, total HVAC thermal energy use was, for south orientation, 84 kWh in the reference cell and 106 kWh in the ZNE cell, representing a 25% increase. The corresponding energy use values for west orientation are 56 kWh, 84 kWh and 49%.

³ Here, “thermal energy use” is used to mean the sum of the thermal (heating and cooling) loads measured in the space with the fan energy use.

The lower cooling thermal energy use in the ZNE cell relative to the reference cell is the cumulative result of 1) reduced internal heat gains from lighting and plug loads that need to be compensated for by the HVAC system and 2) the more efficient operation of the HVAC system in the ZNE cell – wider deadband and setbacks/shutoff when the space was deemed unoccupied – as well as 3) the presence of MSDs in the ZNE cell. However, despite the more efficient HVAC operation and MSDs, the reduced internal heat gains in the ZNE cell also result in increased heating thermal energy use.

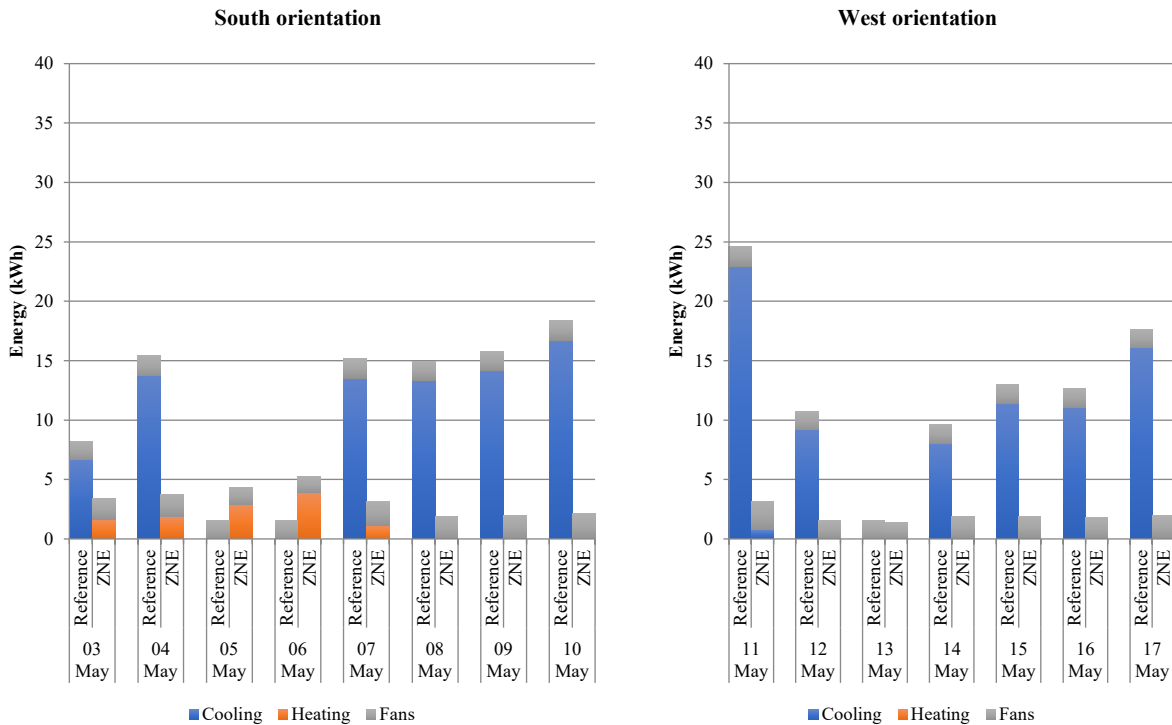


Figure 16. Daily cooling load, heating load, and fan energy consumption during Test 1 (May).

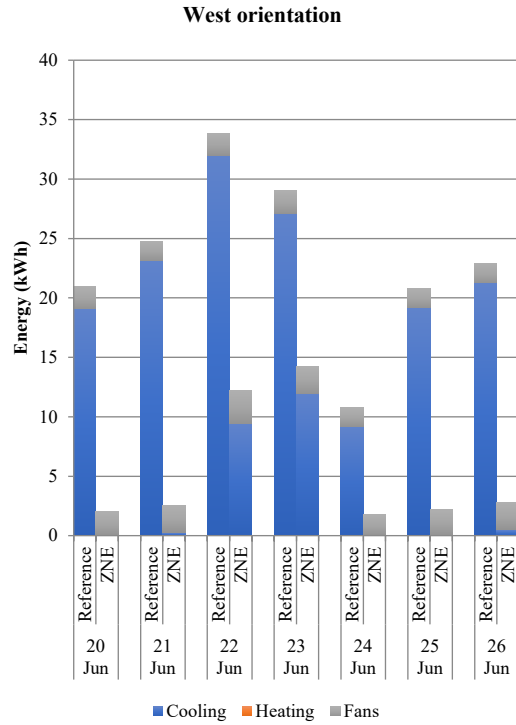
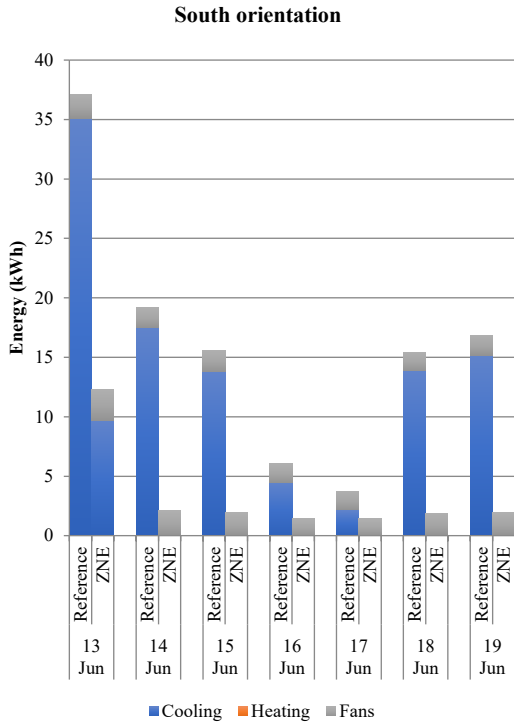


Figure 17. Daily cooling load, heating load, and fan energy consumption during Test 2 (June).

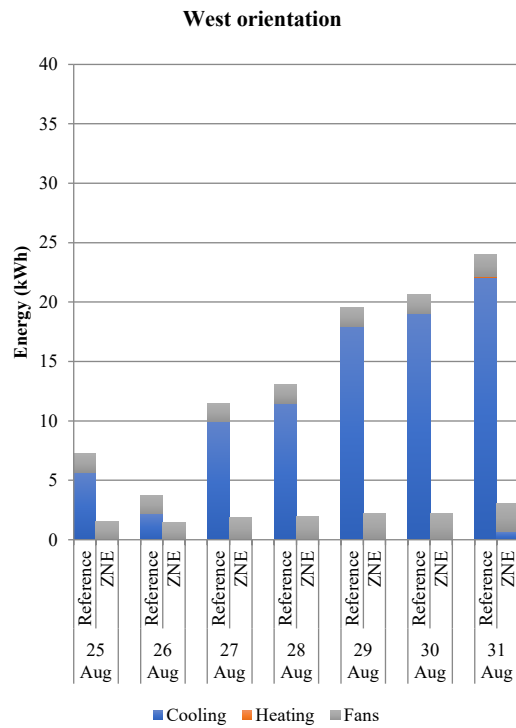
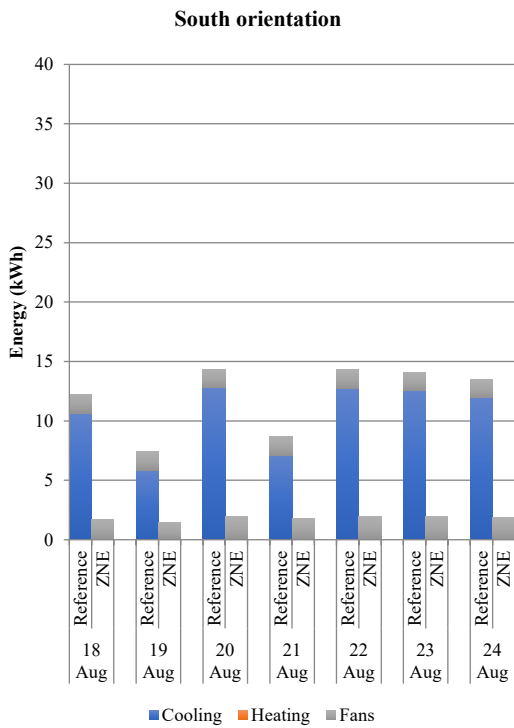


Figure 18. Daily cooling load, heating load, and fan energy consumption during Test 3 (August).

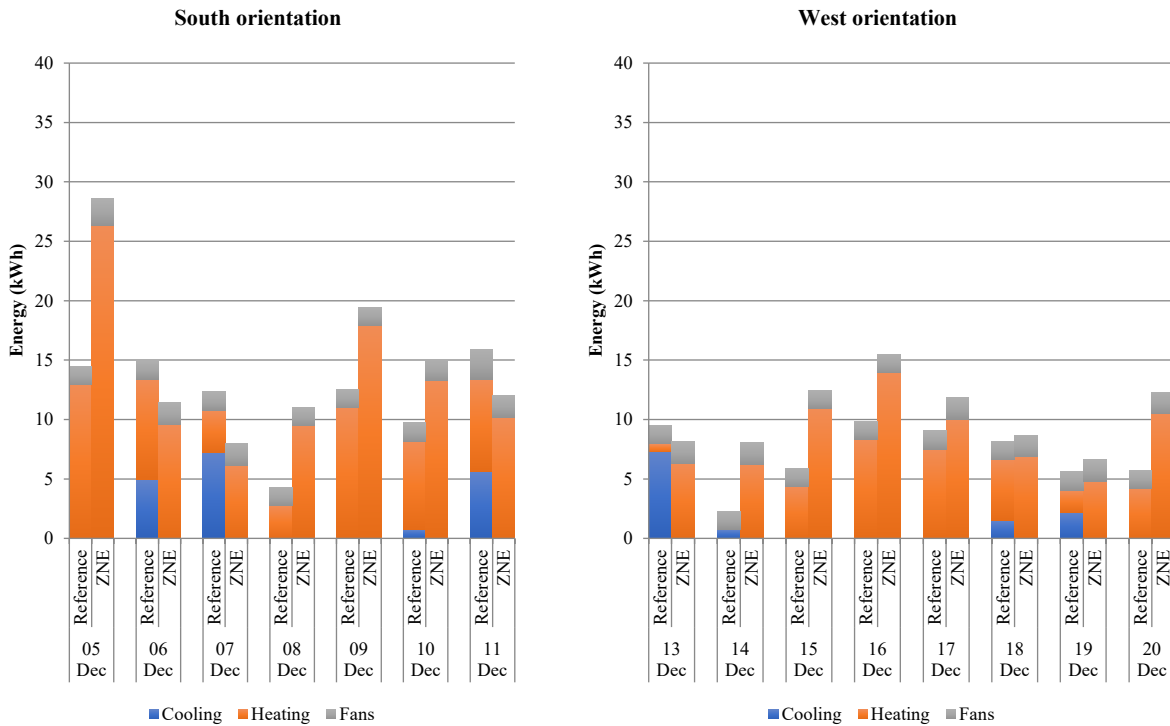


Figure 19. Daily cooling load, heating load, and fan energy consumption during Test 4 (December).

3.1.3.2 Energy use

This subsection shows results from the calculations of site energy using the measured levels of thermal energy detailed in the previous subsection. Figure 20 to Figure 23 show daily energy use for each of the four testing periods. The most remarkable difference between these calculated energy use values and the measured thermal energy values is that, once HVAC equipment efficiency is taken into account, the amount of energy required for heating the ZNE cell increased significantly; this is mainly due to the fact that it is assumed that the ZNE cell is heated by a heat pump (for a zero-carbon approach), unlike the reference cell, which is assumed to be heated by a gas furnace. It is also noticeable that, for the ZNE cell, results show more efficient cooling than for the reference cell. For example, for June 23, the measured cooling thermal energy use (Figure 17) in the ZNE cell is 44% of that in the reference cell (11.95 versus 27.08 kWh) whereas the corresponding ratio for calculated electricity use (Figure 21) is only 28% (3.09 versus 11.13 kWh for the ZNE and reference cells, respectively). This is due not only to the greater efficiency of the cooling system assumed for the ZNE cell, but also to the lower cooling loads present in the cell due to internal gain reduction, which consequently allows the space to be cooled more frequently just through the use of the economizer, when the outside air is at a sufficiently low temperature. In contrast, a space with higher internal gains would in some cases require additional cooling energy expended through the compressor-based system, expending substantially more energy.

For May, June and August combined, calculated HVAC energy use was 115 and 59 kWh in the reference and ZNE cells respectively, for south orientation, resulting in a savings of 49%; the corresponding values for west orientation were 133 kWh, 50 kWh and 63%. During the

December test, HVAC energy use with south orientation was 85 kWh and 120 kWh for the reference and ZNE cells, respectively; a 41% increase; the corresponding values for west orientation were 56 kWh, 99 kWh and 77%.

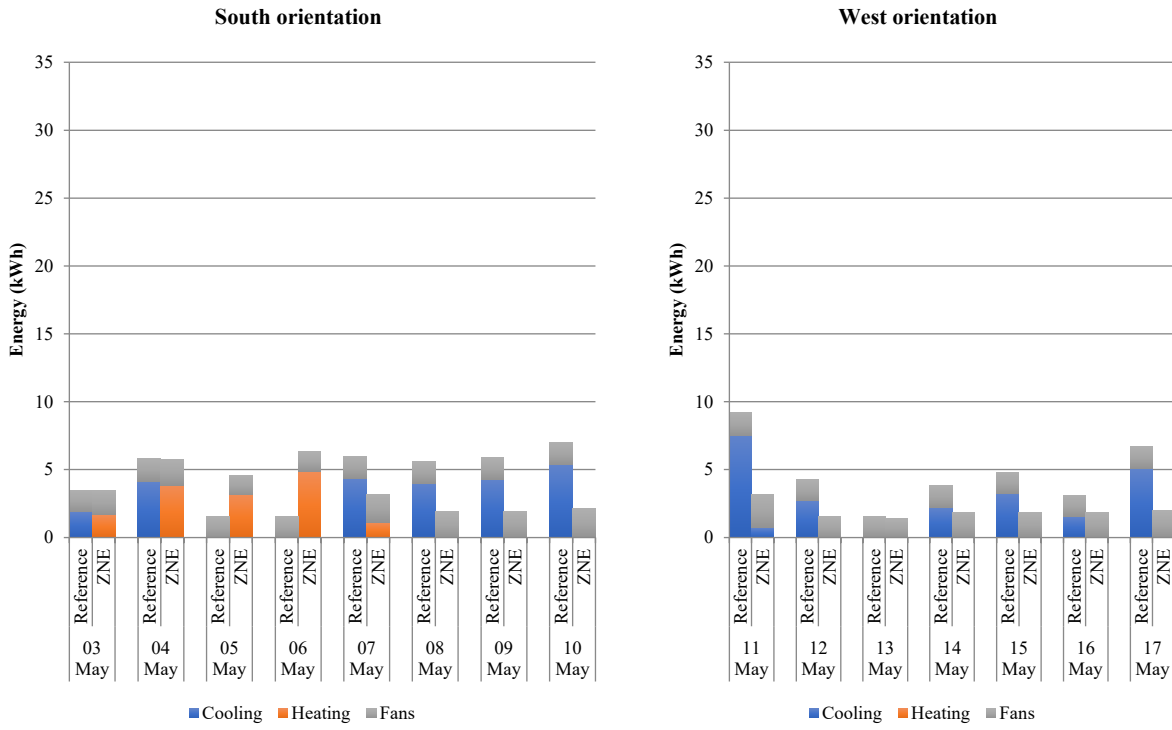


Figure 20. Daily HVAC energy consumption during Test 1 (May).

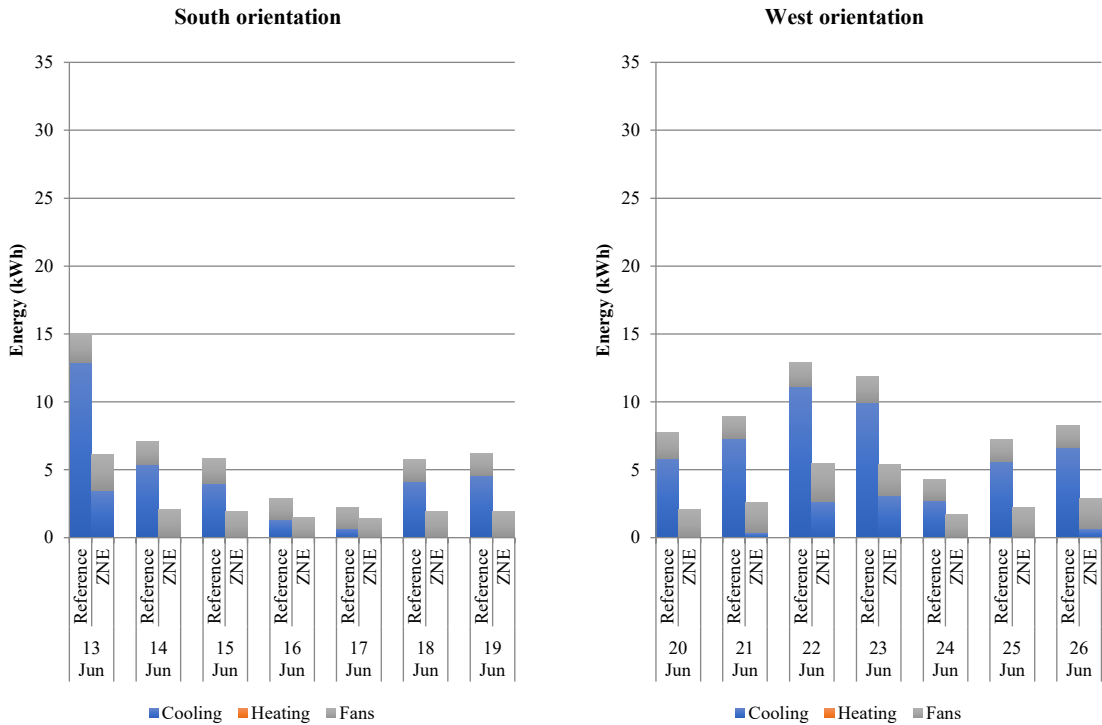


Figure 21. Daily HVAC energy consumption during Test 2 (June).

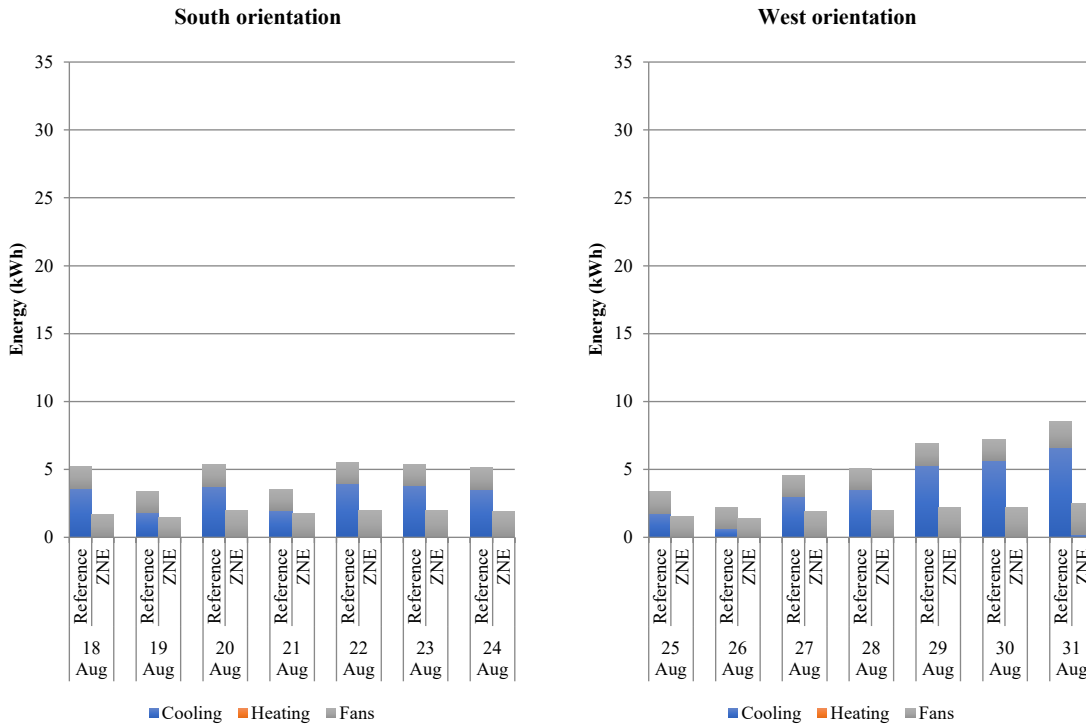


Figure 22. Daily HVAC energy consumption during Test 3 (August).

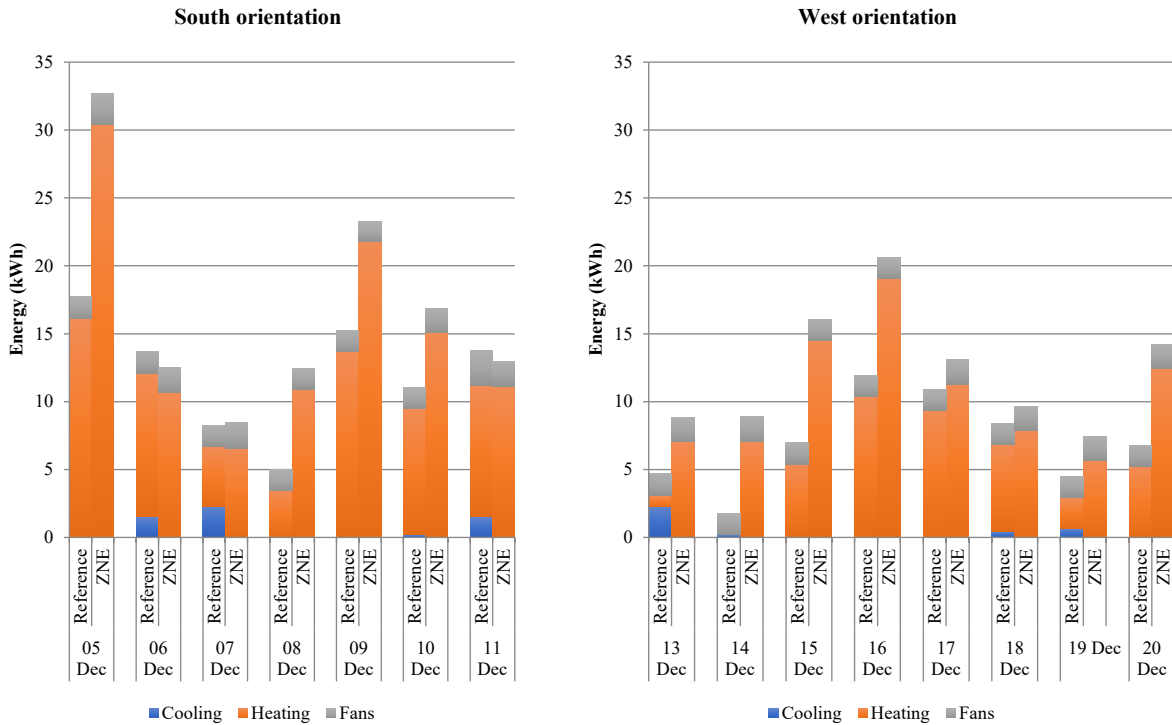


Figure 23. Daily HVAC energy consumption during Test 4 (December).

3.1.4 Total energy use

Total energy consumption, calculated by adding calculated HVAC energy use and measured lighting and plug load energy use, is shown in Figure 24 to Figure 27. ZNE package savings were in the 59%-69% range for cooling-prevalent test periods and 22-25% range during heating-prevalent test periods. Overall, the ZNE package results in substantial reductions in energy use, with particularly high savings for periods during which cooling is the main mode of HVAC operation. For periods during which heating is more prevalent, the savings picture is more mixed because the ZNE package will use more energy for heating than the reference condition; these tests show, however, the reductions in plug load and lighting energy use can more than compensate for this increase. Furthermore, this increase does not necessarily have a proportionate impact on carbon emissions because in the ZNE approach heating is done using electricity – which can come from local or more remote renewable sources – rather than through fossil fuel (natural gas) burning done locally as assumed for the reference condition.

When consulting a database for ZNE office buildings (New Buildings Institute, 2022) in the same geographical area (San Francisco Bay Area, United States) of the facility where the experiment was conducted, annual energy use intensity (EUI) for buildings verified to have achieved zero-net energy consumption varies between 22 and 158 kWh/m². For cooling-prevalent periods, the annualized total EUI for the ZNE cell was 46 and 41 kWh/m² for South and West orientations, respectively. The equivalent numbers for heating-prevalent periods are 132 and 107 kWh/m². Although the exact levels would depend on the particular mix of heating and cooling for a particular building, results indicate that the retrofit package evaluated in this experiment would enable achieving energy performance well within the range for ZNE buildings in a similar climate.

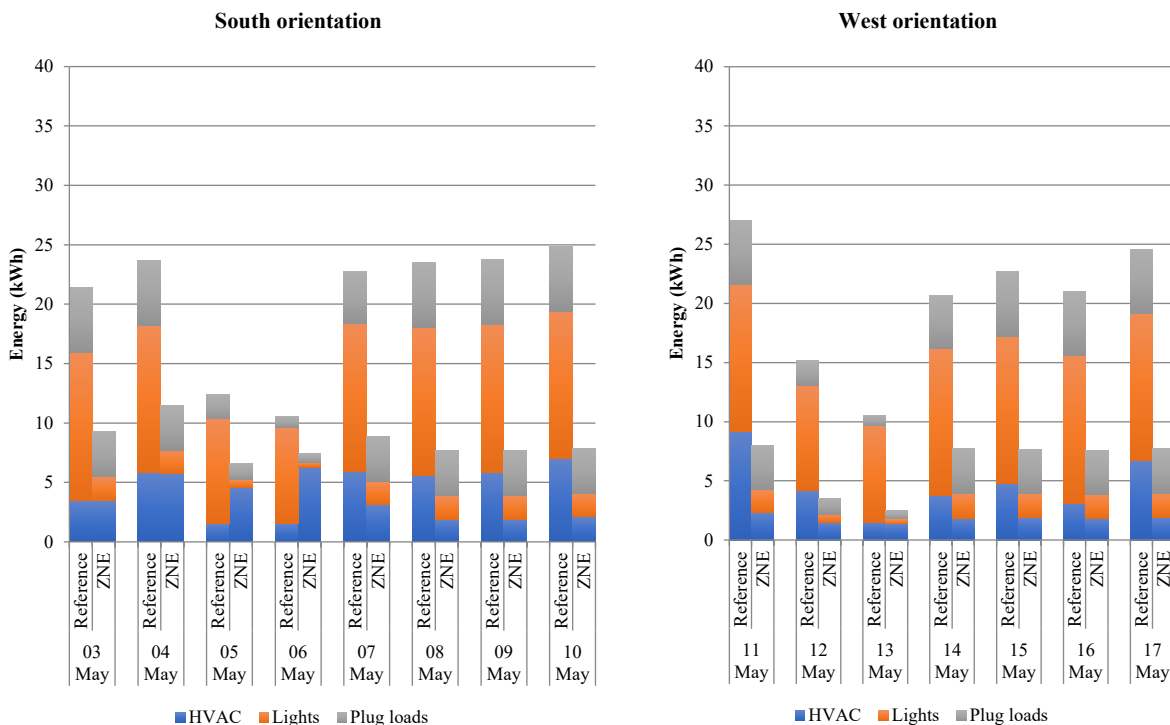


Figure 24. Total energy consumption during Test 1 (May)

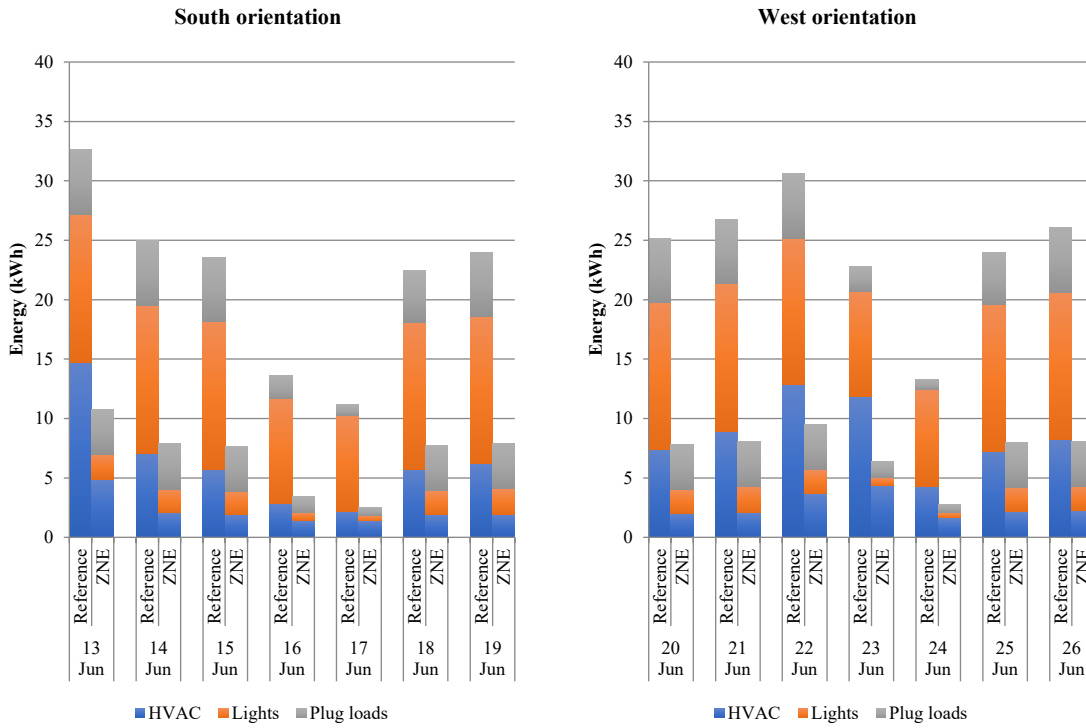


Figure 25. Total energy consumption during Test 2 (June)

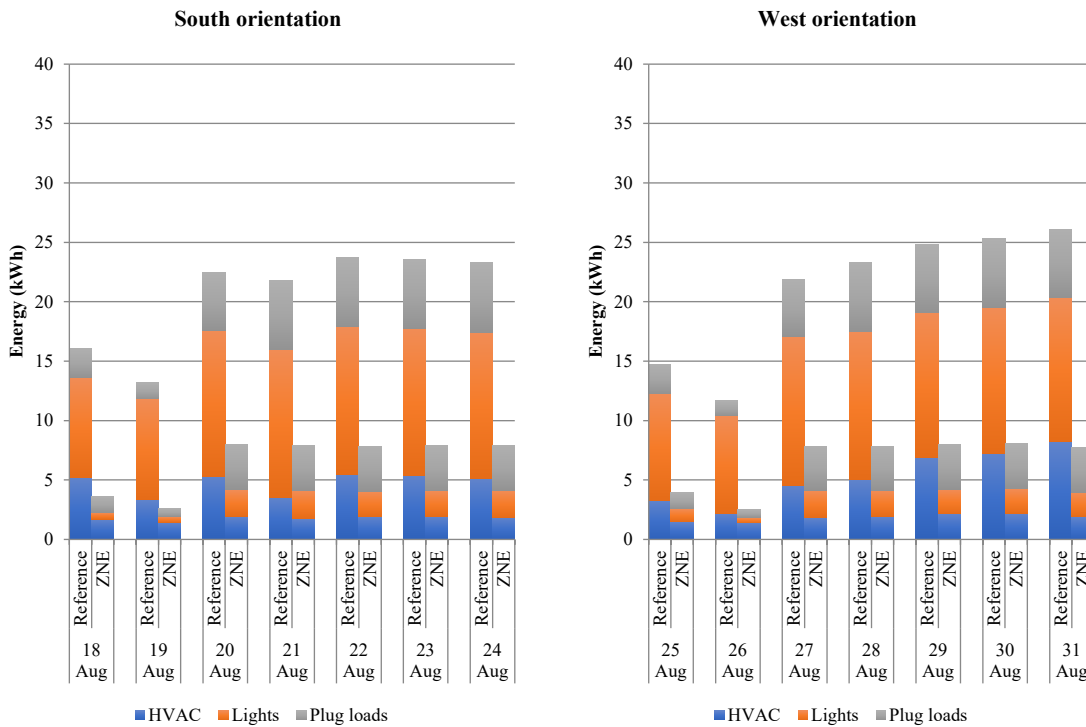


Figure 26. Total energy consumption during Test 3 (August)

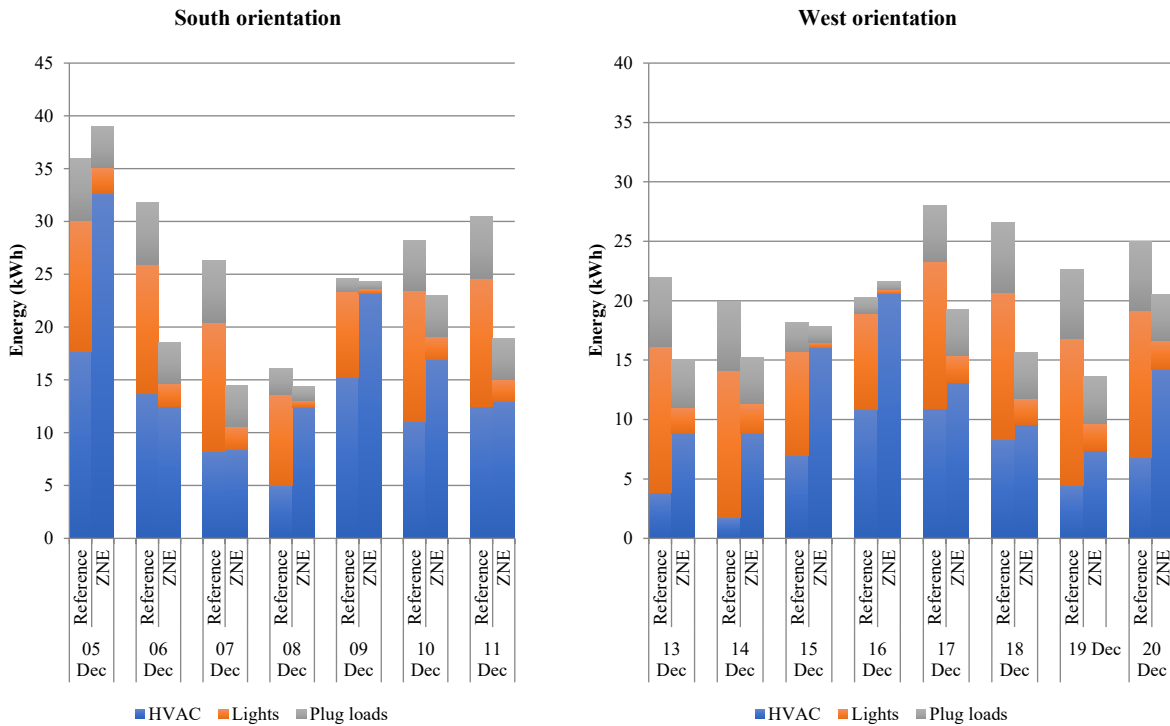


Figure 27. Total energy consumption during Test 4 (December)

3.2 Indoor environmental quality

3.2.1 Thermal comfort

For weekdays and between 8 AM and 6 PM, Figure 28 and Figure 29 show PMV and PPD values for the four tests. It is noticeable that the spread in PMV tends to be larger for the ZNE cell than for the reference cell; this is most probably related to the wider deadband used for temperature control in the ZNE cell.

For the cooling season tests (May, June, and August), the ZNE cell appears to be warmer than the reference cell, with what appears to be some overcooling in the window space of the reference cell (PMV in the -0.5 to -1 range). Correspondingly, PPD in that space spends a significant amount of time above the 20% limit, whereas in other spaces it is mostly in the recommended range. During the heating season (December), the ZNE cell appears cooler than the reference cell, with the window space frequently in the -0.5 to -1 (“slightly cool”) PMV range. Again, this is also reflected in frequent PPD values above 20%. Here it is possible that the single-pane window plays a part in making the space less comfortable than it would be with a better insulating window, such as a low-emissivity double-pane window.

All in all, the ZNE package can be said to maintain acceptable levels of thermal comfort for a substantial amount of time, with the possible exception of areas near single pane windows during the heating season. This might be mitigated by retrofitting windows to be more insulating, or by using any shading devices that reduce the convective movement of air close to the window.

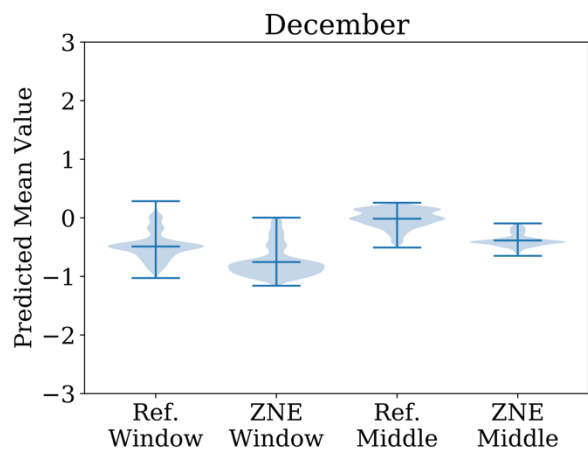
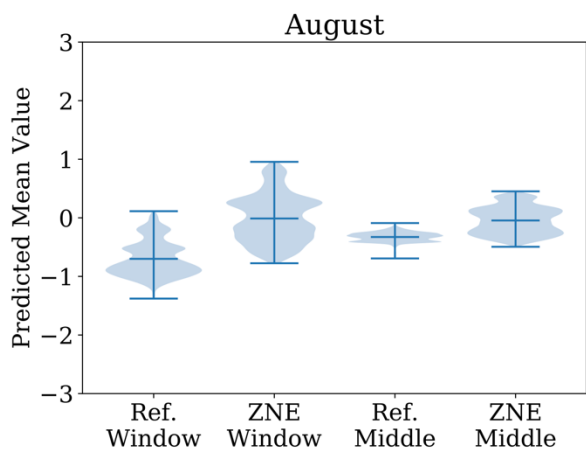
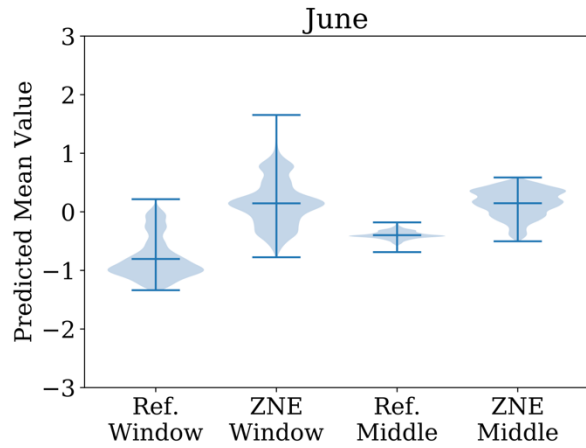
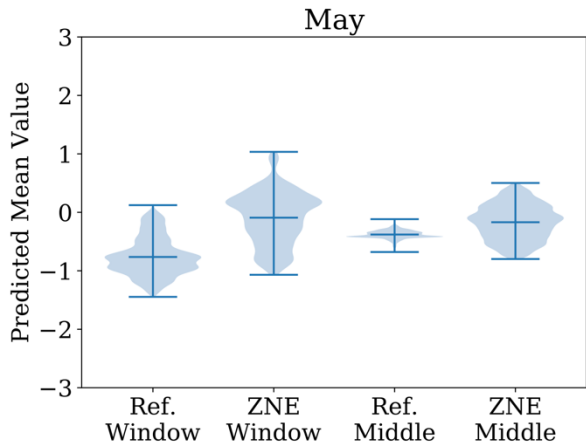
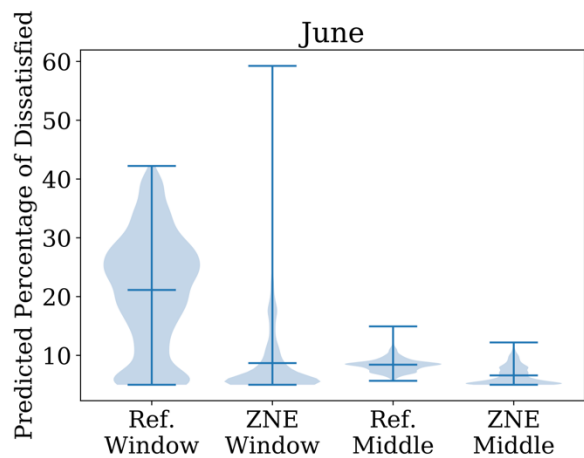
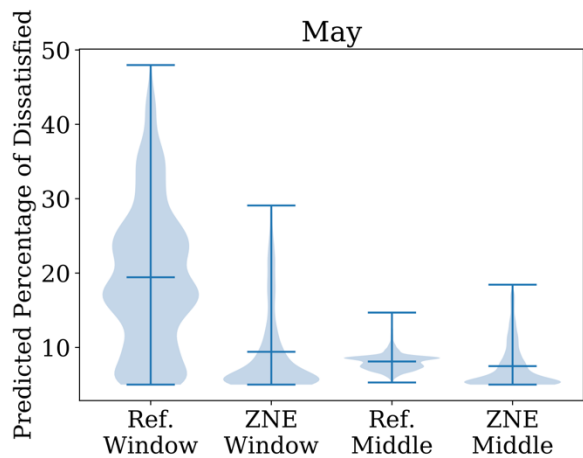


Figure 28. Kernel-density estimator distribution plots of Predicted Mean Value for each of the four tests. Each plot contains the distribution for the window and middle spaces both in the reference and in the ZNE cells.



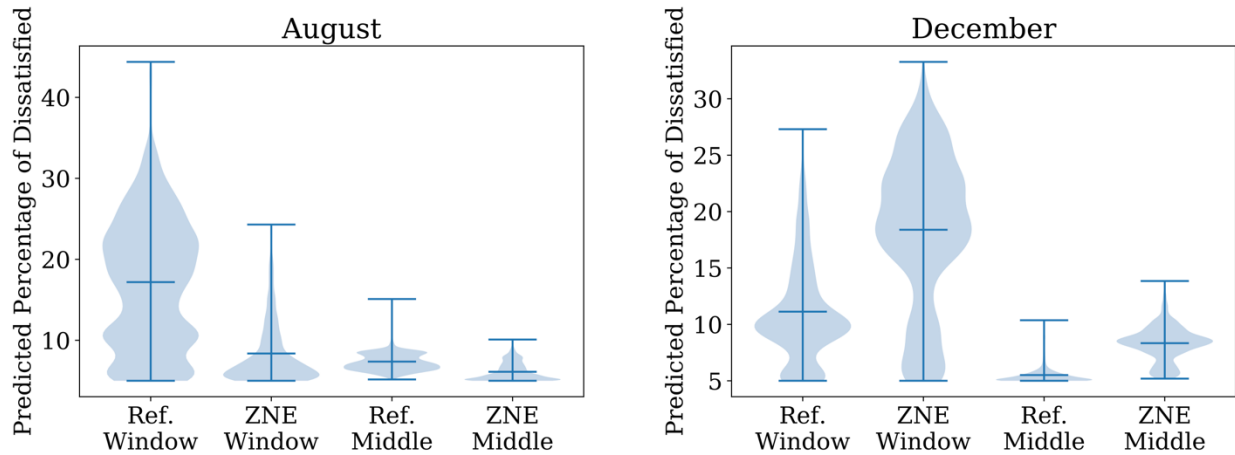
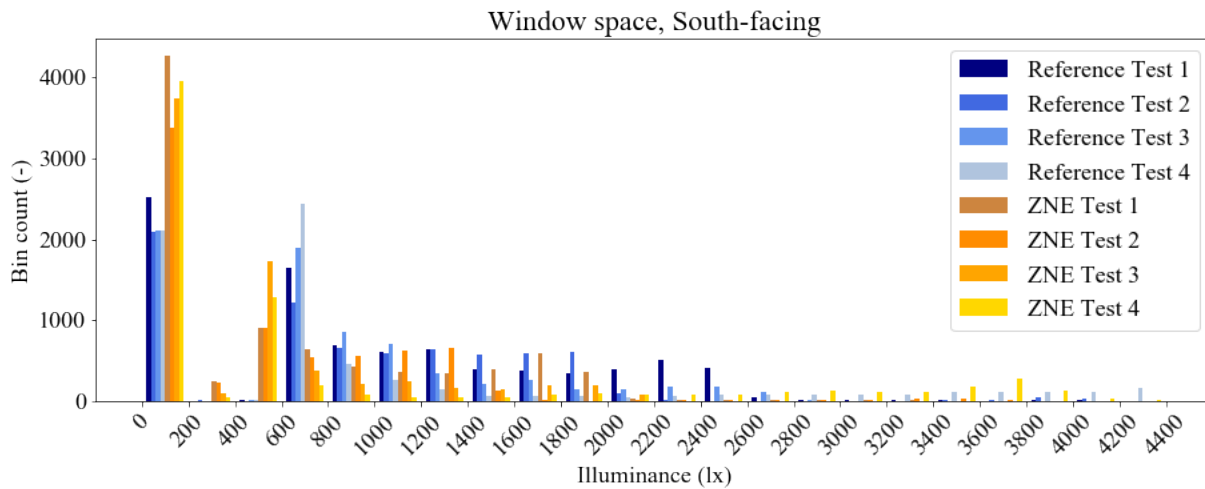


Figure 29. Kernel-density estimator distribution plots of Predicted Percentage of Dissatisfied for each of the four tests. Each plot contains the distribution for the window and middle spaces both in the reference and in the ZNE cells.

3.2.2 Light levels

Histograms of the average horizontal illuminance in each space are shown in Figure 30 for weekday data only and south orientation (similar plots for west orientation are given in the Appendix). When lights were on, light levels in the ZNE cell were generally adequate, above 400 lx for the window space, in the 200-400 lx range for the middle space, and in the 400-600 lx range for the back space. In that cell, occupancy controls meant that the lights were off (represented in the histograms by the 0-200 lx range) for longer periods than in the reference cell.



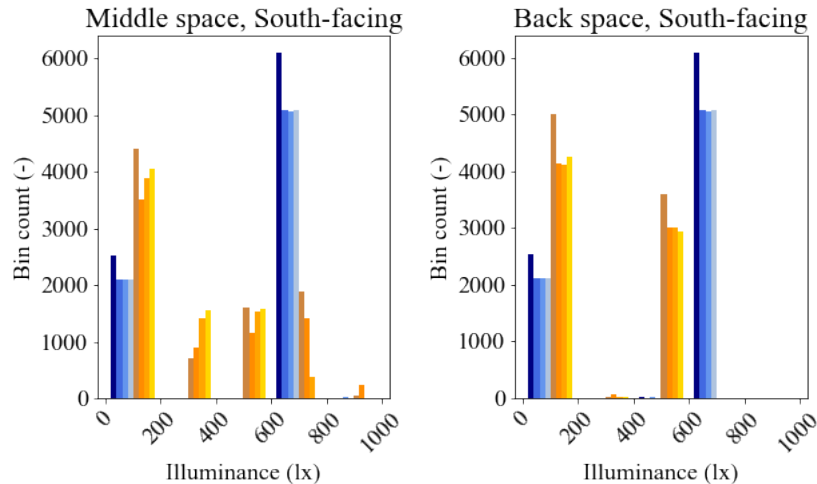


Figure 30. Average illuminance frequency of one-minute timesteps during weekdays by space, with south-facing orientation.

3.2.3 Visual Comfort

In the middle space of the both ZNE and reference cells⁴, measured DGP was well below the 0.35 threshold for perceptible glare. In the ZNE cell, for the measuring position that had the TDD in its field of view, DGP stayed under 0.25 for the whole period (see Figure 31 for an example; a more complete set of results is included in the Appendix). For the other measuring position in the middle space of the ZNE cell (which did not have the TDD in its field of view), as well as for both measuring positions in the middle space of the reference cell, DGP values were consistently below 0.15 for the duration of the study.

In the window spaces of both cells no significant differences were observed between cells in measured DGP. In May, June and August, when the cells were facing south, maximum DGP was in the vicinity of 0.35 facing the window (see Figure 32 for an example), and in the 0.25-0.30 range when facing one of the side walls. When the cells were facing west, DGP was in the 0.45-0.55 range for 2-3 hours in the afternoon whenever the weather was sunny, indicating the likelihood of disturbing or even intolerable glare. In December, measured DGP with cells facing south peaked near 0.55 for measurements facing the window, and was in the 0.35-0.40 range for measurements facing one of the side walls; with the cells facing west, maximum DGP measured was in the 0.30-0.40 range for measurements facing the window and around 0.30 for measurements facing one of the side walls.

⁴ DGP was developed to quantify glare probability from daylight sources. Strictly speaking it does not apply to the middle space of the reference cell, since that space does not contain daylight sources; the same goes for the position in the middle space of the ZNE cell that did not have the TDD in its field of view. These results are mentioned here and included in the Appendix for illustrative purposes only.

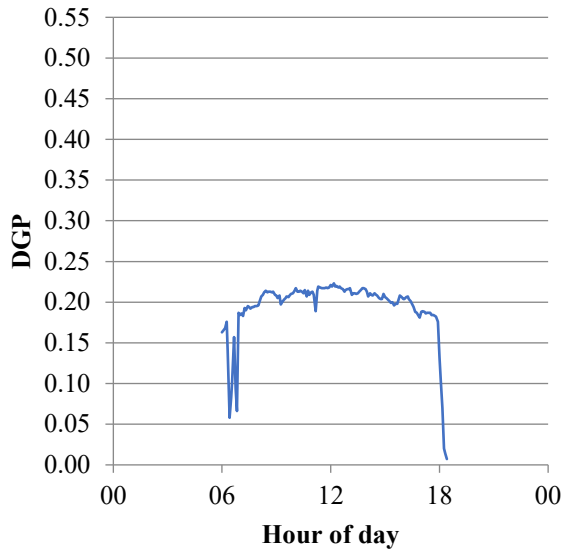


Figure 31. DGP in the middle space of the ZNE cell for a typical day during Test 1 (May), with South orientation. Only this orientation is shown because DGP results in this space did not vary significantly with orientation.

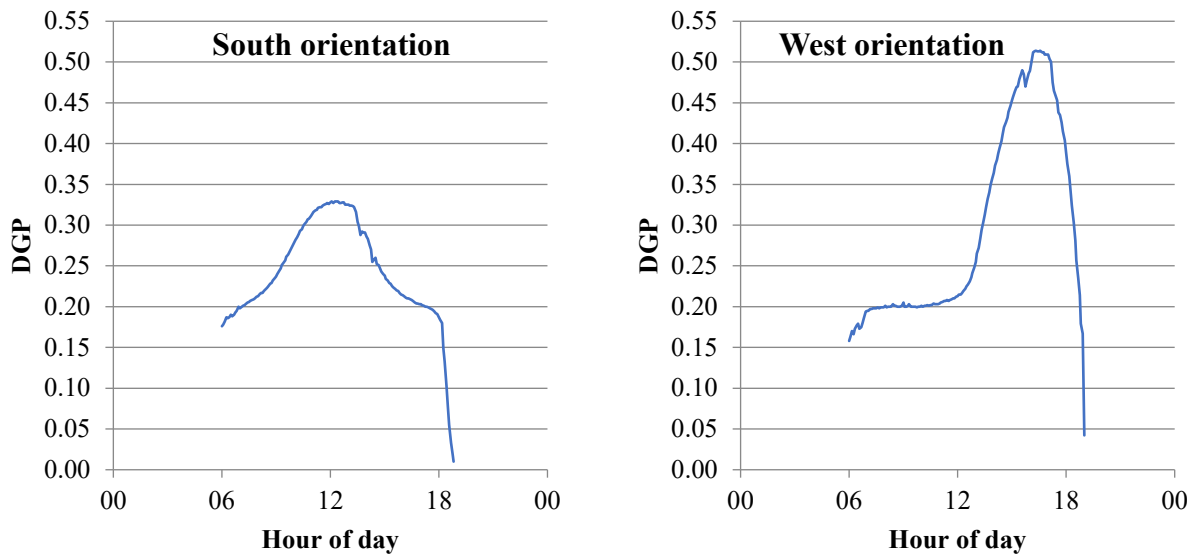


Figure 32. DGP facing the window in the window space of the reference cell for typical days during Test 1 (May) for south and west orientation.

4 Discussion

While experimental studies are ultimately more realistic, e.g., when compared to simulation, they can raise questions about their applicability beyond the particular weather conditions that were present during the experiment. To illustrate how variations in outside air temperature might affect energy performance, Figure 33 shows a plot of average hourly heating and cooling energy use versus average hourly outside air temperature. It is apparent from the figure that, while the ZNE cell is at a disadvantage for low (below 10°C) outside air temperatures, that is offset by a clear advantage as temperature increases. The annual balance of energy savings for

a particular building will depend on the annual distribution of outside air temperatures at the building's location. In addition, carbon emissions are increasingly becoming a strong factor in determining suitable retrofit measures and while a carbon emissions evaluation was not conducted with this work it is fair to assess that the ZNE package would easily outperform the reference case due to the fact that natural gas is the primary source of heating for the reference case, as opposed to the ZNE package and its all-electric heat pump.

This study was conducted in a location with Mediterranean climate and therefore its results are most applicable in areas of the globe with comparable climates, such as Southern Europe, parts of North Africa, and western coastal areas in Australia, South Africa, and North and South America, some of which are significantly populated. While it was not a primary goal of this study to extrapolate experimental performance for different climates – achieving an equivalent set of results would be best achieved by performing the same experiment in other locations – the cooling and heating trends versus temperature that Figure 33 shows indicate that the package evaluated in this study would be generally suitable for climates without significant need for heating; in those climates, the ZNE package's advantages in reduced cooling energy use would be realized during most of the year or all year. As climates become, on average, warmer over the next decades, the areas of the globe where this applies are likely to expand even further.

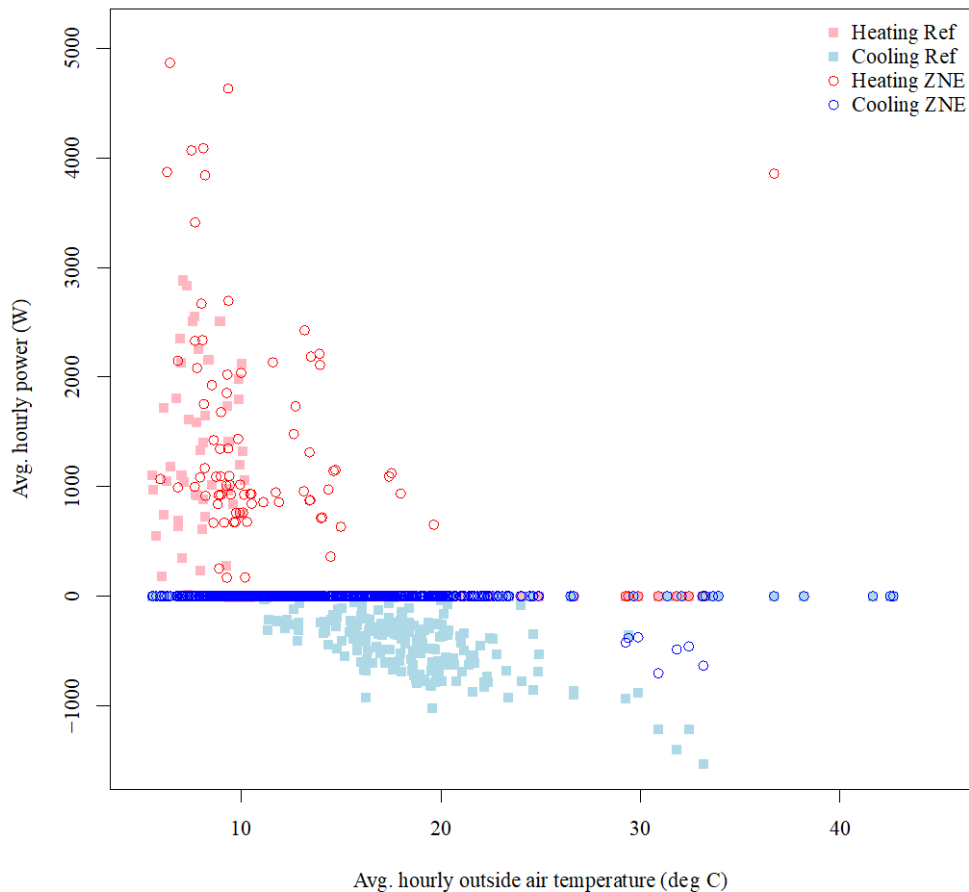


Figure 33. Average hourly heating and cooling power for each cell, plotted against the average hourly outside air temperature. Data shown is for all four tests with south orientation.

5 Conclusions

This paper presents a real-time, side-by-side experimental validation of ZNE retrofit packages for small commercial buildings. Evaluating retrofit solutions is important for addressing the climate crisis in areas of the globe where building replacement rates are low. The ownership structure of small commercial buildings poses a particular challenge for retrofits because of limited resources for identifying, analyzing, and procuring measures for reducing energy use; one solution that minimizes costs and disruptions to building operations is to define bundles of energy efficiency measures that can be installed in a single event. A real-time, side-by-side experimental evaluation in controlled conditions avoids the drawbacks of both field studies in operating buildings, which are often limited by the necessity of a pre-/post-installation design and by the need to not disturb building operations, and simulation studies, which provide useful information about potential performance but can be limited by idealized assumptions about building construction and operation.

The results from this experiment indicate that the proposed ZNE package can save significant amounts of energy for small commercial buildings during both cooling- (59%-69%) and heating-prevalent (22%-25%) periods, despite a HVAC energy penalty during the latter. Lighting energy savings was 85% (a reduction from 190 to 28 Wh/m² per day) regardless of orientation. Plug load energy savings was 31% (a reduction from 73 to 51 Wh/m² per day), also independent from orientation. These internal load savings were in line with the differences in plug load and lighting power densities between reference and ZNE cells. During cooling-prevalent periods, total energy savings were 65% for south orientation and 68% for west orientation; during heating-prevalent periods total energy savings were 22% for south orientation and 25% for west orientation. During cooling-prevalent periods, measured HVAC thermal energy savings were 79% for south orientation and 81% for west orientation; the corresponding values for heating-prevalent periods are -25% and -49%, respectively. These differences between the reference and ZNE cells result from the cumulative effects of reduced internal heat gains from lighting and plug loads, a more efficient operation of the HVAC system and presence of MSDs in the ZNE cell. In terms of calculated actual HVAC energy use, for cooling-prevalent periods savings were 49% for south orientation and 63% for west orientation; the corresponding values for heating-prevalent periods are -41% and -77%, respectively. Besides the factors mentioned above, these results reflect the different heating systems assumed for each cell (heat pump and gas-fired furnace for ZNE and reference cells, respectively).

The ZNE cell tended to have a wider range in thermal sensation levels (Predicted Mean Value) than the reference cell, and tended to be warmer than the reference cell during the cooling season and cooler during the heating season. Thermal comfort conditions were generally comparable in the interior spaces of the two cells. Regarding the window space, the reference cell was slightly too cool during the cooling season and the ZNE cell was slightly too cool during the heating season; some of this could be mitigated by improvements to the windows and/or shading devices. Overall, there were no inordinate differences in thermal comfort between the

two cells. The occurrences of probable glare that were measured were not related to the ZNE package; they are mainly related to the nature of the shading device selected from the window – a generic, white venetian blind representative of what might be installed in many existing small commercial buildings; there was no significant difference between the ZNE and reference cells in this regard. A blind with darker, or thicker slats would probably have provided better glare control. While this might result in negative impacts on daylight availability in the spaces adjacent to the window, with corresponding impacts on lighting energy savings, measuring those impacts was not in the scope of the work presented in this paper.

While the discussion section in this paper broaches the applicability of these experimental results to other locations, further experimental evaluations of similar or identical packages in other locations with similar but not identical climates would provide further confidence in the wide applicability of this type of ZNE retrofit package. Also of interest for further research is the development and evaluation of ZNE retrofit packages for small commercial buildings in areas with significant heating requirements.

6 Acknowledgements

The authors wish to acknowledge LBNL colleagues Christian Fitting, Daniel Fuller, Joshua Mouldoux, and Ari Harding for their invaluable contributions in setting up and maintaining the experiment; Eleanor Lee and Christoph Gehbauer for access to solar data; Jordan Shackelford for discussions on activating luminaire occupancy sensors; Kaiyu Sun for questions on EnergyPlus modeling. The authors also acknowledge John Bruschi at Integral Group for assistance with the EnergyPlus model.

This work was supported by the California Energy Commission through its Electric Program Investment Charge (EPIC) Program on behalf of the citizens of California and by the Assistant Secretary for Energy Efficiency and Renewable Energy of the U.S. Department of Energy under Contract No. DE-AC02-05CH11231.

7 References

- Acutherm, 2020. Thermafuser TF-HC VAV Diffuser [WWW Document]. URL <https://acutherm.com/product/tf-square-therma-fusertm-vav-diffuser/> (accessed 10.10.20).
- Akimoto, T., Tanabe, S., Yanai, T., Sasaki, M., 2010. Thermal comfort and productivity - Evaluation of workplace environment in a task conditioned office. *Build. Environ.* 45, 45–50. <https://doi.org/10.1016/j.buildenv.2009.06.022>
- ASHRAE, 2013. Thermal Environmental Conditions for Human Occupancy, ANSI/ASHRAE Standard-55-2013.
- ASHRAE, 2008. 90.1 User's Manual, ANSI/ASHRAE/IESNA Standard 90.1 - 2007.
- ASHRAE, 2001. Handbook of Fundamentals. American Society of Heating, Refrigerating and Air-Conditioning Engineers, Atlanta, GA.

- California Energy Commission, 2015. 2016 Building Energy Efficiency Standards for Residential and NonResidential Buildings (No. CEC-400-2015-037-CMF). California Energy Commission.
- Chidiac, S.E., Catania, E.J.C., Morofsky, E., Foo, S., 2011. Effectiveness of single and multiple energy retrofit measures on the energy consumption of office buildings. *Energy* 36, 5037–5052. <https://doi.org/10.1016/j.energy.2011.05.050>
- Dean, E., Turnbull, P., 2014. Zero Net Energy Case Study Buildings, Vol. 1. Pacific Gas and Electric Company.
- EnergyPlus, 2018. EnergyPlus Engineering Reference.
- FLEXLAB, Lawrence Berkeley National Laboratory, 2020. FLEXLAB [WWW Document]. URL <https://flexlab.lbl.gov> (accessed 10.9.20).
- Henderson, S., Mattock, C., 2007. Approaching Net Zero Energy in Existing Housing (Research Report). Canada Mortgage and Housing Corporation.
- Hu, M., Milner, D., 2021. Factors influencing existing medium-sized commercial building energy retrofits to achieve the net zero energy goal in the United States. *Build. Res. Inf.* 49, 525–542. <https://doi.org/10.1080/09613218.2020.1798208>
- Lee, S.H., Hong, T., Piette, M.A., Taylor-Lange, S.C., 2015. Energy retrofit analysis toolkits for commercial buildings: A review. *Energy* 89, 1087–1100. <https://doi.org/10.1016/j.energy.2015.06.112>
- Malet-Damour, B., 2019. Photometrical analysis of mirrored light pipe_ From state-of-the-art on experimental results (1990–2019) to the proposition of new experimental observations in high solar potential climates. *Sol. Energy* 17.
- Mathew, P., Regnier, C., Shackelford, J., Walter, T., 2020. Energy Efficiency Package for Tenant Fit-Out: Laboratory Testing and Validation of Energy Savings and Indoor Environmental Quality. *Energies* 13, 5311. <https://doi.org/10.3390/en13205311>
- New Buildings Institute, 2022. Getting to Zero Buildings Database [WWW Document]. URL <https://newbuildings.org/resource/getting-to-zero-database/> (accessed 4.24.22).
- New Buildings Institute, 2021. Zero Energy Case Studies [WWW Document]. URL <https://newbuildings.org/hubs/zero-energy/#case-studies> (accessed 10.9.21).
- Regnier, C., Fernandes, L., Sun, K., Bruschi, J., 2020. ZNE for All! Enabling Zero Net Energy Retrofits for Small Commercial Offices. Presented at the 2020 ACEEE Summer Study on Energy Efficiency in Buildings, p. 19.
- Regnier, C., Harding, A., Robinson, A., 2015. Achieving a Net Zero Energy Retrofit – in a humid, temperate climate – lessons from the University of Hawai’i at Mānoa (No. LBNL-189802). Lawrence Berkeley National Laboratory.
- Regnier, C., Sun, K., Hong, T., Piette, M.A., 2018. Quantifying the benefits of a building retrofit using an integrated system approach: A case study. *Energy Build.* 159, 332–345. <https://doi.org/10.1016/j.enbuild.2017.10.090>
- Shackelford, J., Mathew, P., Regnier, C., Walter, T., 2020. Laboratory Validation of Integrated Lighting Systems Retrofit Performance and Energy Savings. *Energies* 13, 3329. <https://doi.org/10.3390/en13133329>
- Sherman, R., Naganathan, H., Parrish, K., 2021. Energy Savings Results from Small Commercial Building Retrofits in the US. *Energies* 14, 6207. <https://doi.org/10.3390/en14196207>

- University of California, Berkeley, 2021. CBE Thermal Comfort Tool [WWW Document]. URL <https://comfort.cbe.berkeley.edu/> (accessed 7.21.21).
- U.S. Energy Information Administration, 2021. Annual Energy Outlook 2021. U.S. Department of Energy.
- U.S. Energy Information Administration, 2020. 2018 Commercial Buildings Energy Consumption Survey: Preliminary Results. U.S. Department of Energy.
- Wienold, J., Christoffersen, J., 2006. Evaluation methods and development of a new glare prediction model for daylight environments with the use of CCD cameras. *Energy Build.* 38, 743–757. <https://doi.org/10.1016/j.enbuild.2006.03.017>
- Zhai, J., LeClaire, N., Bendewald, M., 2011. Deep energy retrofit of commercial buildings: a key pathway toward low-carbon cities. *Carbon Manag.* 2, 425–430. <https://doi.org/10.4155/cmt.11.35>